MODELLING AND OPTIMIZATION OF MULTI-AXIS MACHINING PROCESS CONSIDERING CNC MOTION LIMITATIONS

by

SAMET BİLGEN

Submitted to the Graduate School of Engineering and Natural Sciences
in partial fulfillment of
the requirements for the degree of
Masters of Science

Sabancı University
January 2016

MODELLING AND OPTIMIZATION OF MULTI-AXIS MACHINING PROCESS CONSIDERING CNC MOTION LIMITATIONS

APPROVED BY:

Prof. Dr. Erhan Budak
(Thesis Supervisor)

Assoc. Prof. Bahattin Koç

Assoc. Prof. Mustafa Bakkal

DATE OF APPROVAL: 28.04.2016

Anneannem'e…

ABSTRACT

MODELLING AND OPTIMIZATION OF MULTI-AXIS MACHINING PROCESS CONSIDERING CNC MOTION LIMITATIONS

SAMET BİLGEN

Industrial Engineering, MSc. Thesis, 2016

Thesis Supervisor: Prof. Dr. Erhan BUDAK

Keywords: Feedrate Scheduling, Lead and Tilt Angles, Process Simulation, Acceleration and Jerk Limitations, Cycle Time

The importance of multi-axis machining processes is increased over the years, especially for industries such as automotive, aerospace, dies and molds, biomedical where the parts have complex surfaces. As the demand for products is increased from these industries, it became crucial to minimize the cycle time to overcome the demand and also reduce the production costs while maintaining or enhancing the part quality. In order to achieve this the dimensional tolerances and a desired surface quality should be inside the acceptance limit while increasing productivity.

The properties of the machine tool such as its own structure, axis drives, drivetrain, axis control limits and axis motor maximum capabilities can be regarded as boundary conditions of the process. The limits for the drives cannot be used at full capacity constantly as the machining process is a highly variable and flexible operation. For instance, sharp maneuvers on the tool path may not be realized at high feedrate values. In some cases, the required motion exceeds the motion capability of the axis drives, i.e. jerk,

acceleration and velocity limitations. In those cases, the CNC unit slows down the motion to synchronize machine axes to keep up within geometrical limits of the required tool path. On the other hand, sometimes the commanded feed rate may not be achieved at some instances of a cycle involving short distances due to limited jerk and acceleration of the axes. These problems reduce the productivity of the operation as well as the quality of the final product.

This thesis presents a new feed-rate optimization algorithm which re-adjusts the rotary axis motions to stay in the acceleration and jerk limits as well as to obtain a better surface quality for the final product in multi-axis machining. All measured velocity, acceleration and jerk limits are given to the algorithm to re-calculate the tool axis vector, such as lead and tilt angles, for minimizing the cycle time and enhancing part surface quality.

As the current studies do not rely on the drive limits for choosing the tool orientation in multi-axis machining, for the first time, the algorithm represented in this thesis optimizes the tool's lead and tilt angles at each Cutter Location (CL) point. The technique used in the study optimizes the tool orientation vector for minimizing the cycle time by observing the acceleration and jerk limits of the axis drives of the machine tool. The unnecessary motions between CL points generated by commercial software can be eliminated by the algorithm and this increases the productivity of the process.

The feasibility of the algorithm and the models in this thesis is presented on an industrial part geometry where the productivity and machined surface quality improvements are demonstrated.

ÖZET

ÇOK EKSENLİ METAL KESME OPERASYONLARININ TAKIM EKSEN VEKTÖRÜ SEÇİMİ VE İLERLEME HIZI DÜZENLEMESİ İLE MODELLENMESİ VE EN İYİLEŞTİRMESİ

SAMET BİLGEN

Endüstri Mühendisliği, Yüksek Lisans Tezi, 2016

Tez Danışmanı: Prof. Dr. Erhan BUDAK

Anahtar Kelimeler: İlerleme Hızı Düzenlemesi, Eğilme ve Yatma Açıları, Süreç Benzetimi, İvme ve Sarsım Limitleri, İşleme Süresi

Çok eksenli talaşlı imalat yöntemlerinin önemi, özellikle otomotiv, havacılık, kalıpçılık ve biyomedikal endüstrileri gibi üretilen parçaların yüzeylerinin karmaşık olduğu sektörler için son yıllarda oldukça artmıştır. Bu sektörlerde üretilen ürünlere talep arttıkça, hem talebi karşılamak hem de üretim maliyetlerini düşürmek için işleme zamanını azalmak çok önemli bir konuma gelmiştir. İşlem zamanının azaltılmasının yanı sıra, üretim toleransları içinde kalmak ve hatta parça kalitesini iyileştirmek de çok güncel ve önemli bir konu olarak görülmektedir. Yüksek kaliteli parça elde etmek için, boyutsal tolerans ve istenen yüzey kalitesi kabul edilebilir sınırlar içinde olmalıdır.

Takım tezgâhın yapısal özellikleri, eksen sürücüleri, tahrik sistemi, eksen kontrol limitleri ve eksen motorlarının maksimum yetenekleri kesme operasyonu için sınır koşulları olarak

görülebilir. Talaşlı imalat sürecinin çok değişken ve esnek bir süreç olduğu göz önünde bulundurulduğunda eksen sürücü limitlerinin her zaman en yüksek kapasitede kullanılamadığı söylenebilir. Gereken hareketin eksen sürücü limitlerini geçtiği bazı koşullarda CNC algoritması gerekli hareketin hızını kısarak istenilen geometrik ve hareketsel tolerans içinde kalabilmektedir. Bu olayın, operasyonun verimliliğini ve parça kalitesini önemli derecede düşürmekte olduğu söylenebilir.

Bu tez, çok eksenli talaşlı imalat işlemlerinde, döner eksen ilerleme hızlarını, eksenlerin maksimum ivme ve sarsım limitleri dâhilinde tekrar düzenleyerek daha yüksek kaliteli yüzeylere sahip parçaların imalatını mümkün kılacak yeni bir algoritma sunmaktadır. Deneyler ve testler sonucunda elde edilen maksimum hız, ivme ve sarsım değerleri algoritmaya verilerek algoritmanın takım eksen değişkenlerini, eğilme ve yatma açılarını, işlem süresini azaltmak ve parça yüzey kalitesini arttırmak için tekrar hesaplaması sağlanmıştır.

Çok eksenli talaşlı imalat işlemlerinde takım eksen yönelme açısı seçiminde güncel çalışmaların tezgâh eksen sürücü limitlerini dikkate almadığı göz önünde bulundurulduğunda bu tezde anlatılan algoritmanın bir ilk olduğunu söylemek mümkündür. Algoritma her bir kesme noktasında (CL) işleme zamanı azaltılması için döner eksenlerin ivme ve sarsım limitlerini göz önünde bulundurarak takım eksen yönelme vektörünü en uygun hale getirmektedir.

Tez kapsamında anlatılan algoritmanın ve modellerin uygulanabilirliği endüstriyel iş parçası geometrileri üzerinde gösterilmiş ve iyileştirmeler sonuçlarla açıklanmıştır.

ACKNOWLEDGMENTS

In the first place, I would like to express my deepest appreciation to my thesis advisor, Prof. Dr. Erhan Budak, for their patient attitude, numerous advices and contributions to me for completing this thesis. I also thank him for not just being my supervisor but also for acting like one of my family members and their affiliative behavior since our conversancy.

I would like to express my sincere gratitude to my thesis co-supervisor L. Taner Tunç, PhD, for their emotional and motivational support, their precious comments and guiding attitude. I should express clearly that; it would be impossible for me to complete this study without their support.

I would like to thank my committee members, Assoc. Prof. Dr. Mustafa Bakkal and Assoc. Prof. Dr. Bahattin Koç for their encouragements and comments.

During the last 5 years of my academic life, my best friend and my future wife Gözde Bulgurcu was always standing by me to support and encourage me. I would like to thank her for her priceless support. I also thank my fellow friends Turgut Köksal Yalçın, Mehmet Albayrak, Hayri Bakioğlu, Deniz Aslan, Ekrem Can Unutmazlar, Cihan Özener, Mert Kocaefe, Zahra Barzegar and Faraz Tehrenizadeh for working together with me and for all the enjoyable times we shared together.

Also, I wish to acknowledge the support received from Maxima R&D members Dr. Emre Özlü, Esma Baytok, Veli Nakşiler, Anıl Sonugür, Ahmet Ergen and Dilara Albayrak.

Finally, I would like to acknowledge my sincere gratitude to my parents Nil and Sadık who make it possible for me to start and continue my academic career and my sister Nisa for her emotional support.

TABLE OF CONTENTS

LIST OF FIGURES

LIST OF TABLES

LIST OF SYMBOLS AND ABBREVIATIONS

a	Acceleration
CAD	Computer Aided Design
CAM	Computer Aided Manufacturing
CNC	Computerized Numerical Control
MRR	Material Removal Rate
CL	Cutter Location
CC	Cutter Contact
CWE	Cutter Workpiece Engagement
f	Feedrate
f_t	Feed per Tooth
j	Jerk
n_t	Number of Teeth
N	Number of Revolutions per Minute
s	Position
v	Velocity

1 CHAPTER 1 – INTRODUCTION

1.1 Introduction

Manufacturing is a value-adding process in which the raw materials are being converted into finished goods that are desired by customer's needs, expectations and specifications. It can be said that machining is one of the most important sub-family of manufacturing processes. Machining is a metal cutting process where a workpiece is being cut by a cutting tool. Unwanted material is being removed in form of small chips to obtain the desired final shape. Thanks to machining processes' high flexibility and accuracy compared to other traditional manufacturing processes such as casting, deformation or consolidation, it became one of the most widely preferred manufacturing technique in the industry.

With the advancement of machining technologies, the production of complicated parts with complex geometries has become feasible. Thus, machining became one of the most widespread manufacturing technology in the industry. To meet the demands of producing complex parts, some machining technologies such as multi-axis machining is developed. It can be said that 3-axis and 5-axis milling technologies became the most widespread multi-axis machining processes. In both of the production methods, various cutting tools such as, flat, tapered or ball end types can be used. In 3-axis machining, X, Y and Z axes can be commanded simultaneously to contour the desired geometry. In general, 3-axis milling systems have 3 linear axes but none of the rotary ones. When 5-axis machining systems are observed, there are 2 more axes which are rotary when compared to 3-axis version. These 2 rotary axes provide the lead and tilt angles for the tool. This additional 2 degrees of freedom, allow the production system to be more flexible when the machined part have geometrical constraints. A typical 5-axis CNC machine tool can be seen in Figure 1-1.

In contrast, while the systems are being more capable of producing complicated parts, they also became more complicated which affect their production speed. First of all, when the complexity of the hardware of the CNC (Computerized Numerical Controller) machine is increased, the agility decreased due to additional weight of the new components. When the mass of the overall system increased, the acceleration capability is decreased and this bring along some constraints for machining process. The second structural constraint for the CNC system is about its nature. After some modal analysis tests, the natural frequency of the machine tool can be calculated. Thus the acceleration of the axes should be in a shape that it would not self-excite the system, so it would not start to vibrate. In such a case, if the structure vibrates, the machined part surface quality will be decreased and it is an undesired situation.

Such constraints force CNC controller to accelerate and decelerate within some boundaries. If the system is too heavy and its drives are not capable of reaching the desired acceleration/deceleration rates, or there is a possibility that the maximum acceleration/deceleration capabilities of the drives can excite the structure, the machining process became slower. Thus the CNC controller is programmed in such a way that there are predefined acceleration and jerk profiles for each axis for preventing the excitation of the system's structural modes. In addition to this the drive capabilities are also a constraint for the motion of the CNC machine tool.

In a multi-axis machining center such as a 5-axis milling machine, there are 3 linear and 2 rotary axes as can be seen at the right hand side of Figure 1-1. The spindle of this specific CNC machine tool has 3 degrees of freedom by 3 linear axes and the table has 2 degrees of freedom by 2 rotary axes. Each of them has different drive systems with different constraints. For instance, if one of the axes is not capable of the desired motion from the CNC machine tool, the velocity of the all other axes are reduced so the dimensional and geometrical tolerances are not exceeded. This affects the whole process in a negative way and the productivity is decreased. However, if the production procedure is planned according to the constraints of the CNC machine tool drive system at the beginning, the process' efficiency can be increased.

In addition to this, there are other challenges that can a CNC machine tool can encounter. For instance, the feedrate interpolator of the CNC machine tool should minimize unwanted feedrate fluctuations for being efficient. Also, discontinuities in the feed profile should be predicted which will decrease the part quality.

As the demand from the machining industry is increased and the systems became more complex, it became crucial to maximize the production speed while preserving or enhancing the quality of the produced part. The main aim of the study represented in this thesis is to minimize the machining duration by looking at the CNC machine tool's characteristics and its drive capabilities. Thus the productivity of the process can be increased. The CNC machine tool's each axis has unique characteristics that effect the process and these has to be considered while generating the feedrate profiles for a specific toolpath which in return gives a more efficient process to the user.

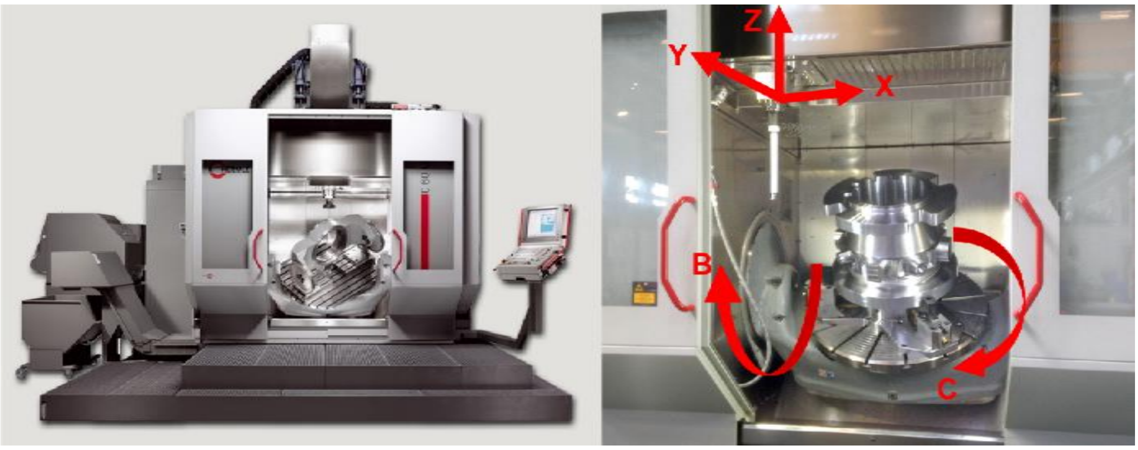

Figure 1-1: A Typical 5-Axis CNC Machine Tool

The machining process has various boundary conditions. The most important ones for maximizing the efficiency and productivity are maximum velocity, acceleration, jerk and force capabilities of the axis drives. In this thesis the proposed method, respects these boundaries to increase the efficiency of the machining process and determines some of the process variables to minimize the required time.

1.2 Definition of Lead & Tilt Angles in 5-Axis Machining Operations

Another boundary condition is about the lead and tilt angles that can be chosen during the machining process. A simple illustration for 5-axis milling process is shown in Figure 1-2. Lead angle is the angle between the machined surface normal and tool orientation's vector component along the cutting direction as can be seen in Figure 1-3. Finally tilt angle is the angle between the machined surface normal and tool orientation's vector component along cross feed direction as can be seen in Figure 1-4.

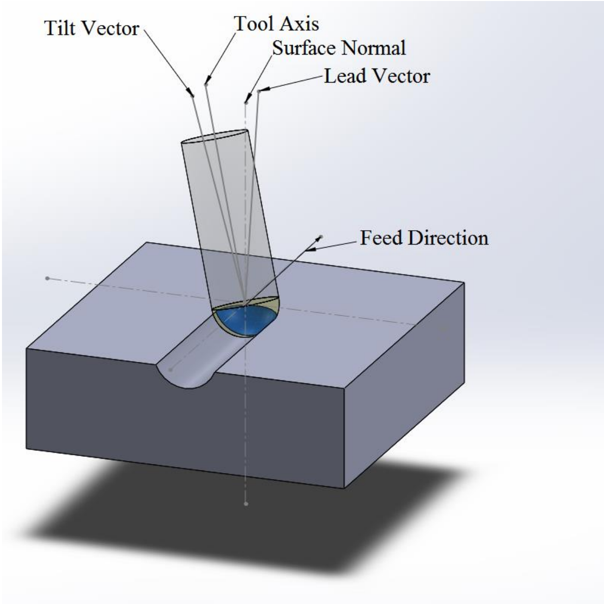

Figure 1-2: Illustration of Lead and Tilt Angles

The approach in this study, which will be explained in the following chapters, looks at the displacement requirements of each axis between two successive control points and tries to minimize the displacement requirement of the slowest axis of a multi-axis CNC machine tool by regarding the maximum capabilities of each axis drive component. The method, uses the data obtained from experimental tests that show the maximum velocity, acceleration and jerk profiles of the axes and re-calculates the optimum lead and tilt angles for minimizing the machining time.

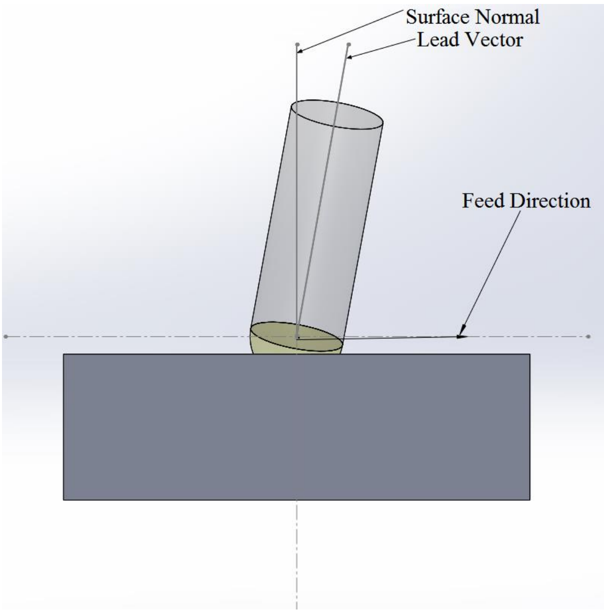

Figure 1-3: Right View of a 5-Axis Milling Operation

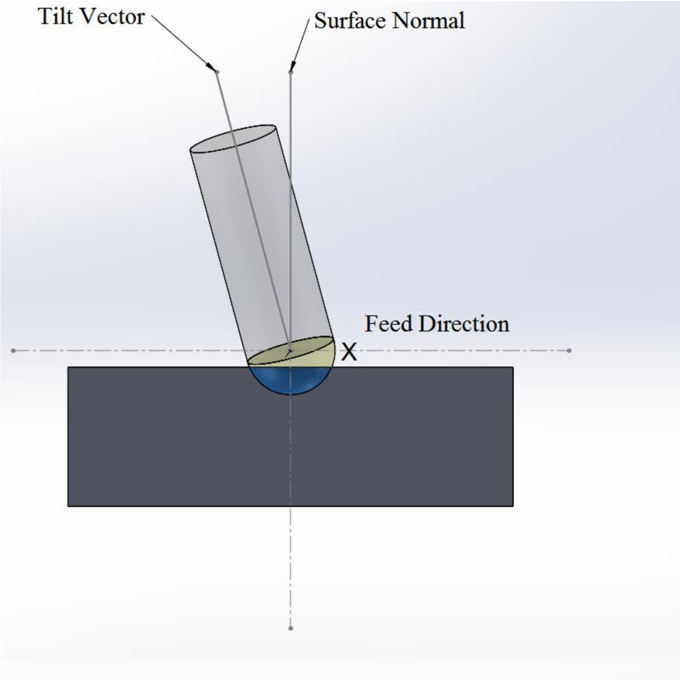

Figure 1-4: Rear View of a 5-Axis Milling Operation

1.3 Problem Definition and Research Objective

General layout for a part design and its production with CNC machine tools consists of five general steps as illustrated in Table 1-1. The first step is the design step in which a part is created with CAD (Computer Aided Design) software and its NC Code is generated with CAM (Computer Aided Manufacturing) software. The NC Code generated consist of only the information about tool path position and feedrate values. The surface or the volume of the part is not included. Additionally, todays CAM software does not include the axis motion characteristics and limits such as jerk and acceleration while creating the NC Code. The negative consequences of this will be discussed in further parts of this thesis. The NC Code being processed by CNC Controller gives the information about axis positions and controller converts it into machine commands. Another important task for CNC Controller is to control the relative motion of each axis between each other and the workpiece. If there is a constraint in the required motion, the controller re-adjusts the command for each axis. This is done by measuring the actuators motions with the feedback provided from positional sensors located in each of the axis, motor and actuators. At the end of the process the final product is formed.

Table 1-1: Production Steps from Design to Final Product

As stated above, the NC Code for a multi-axis machining process is being generated without any information about the axis drive capabilities such as its maximum acceleration or jerk limits. Due to the absence of such information, the commanded feedrate may not be feasible at each block of the NC Code. When an axis is incapable of executing the required motion, CNC controller reduces the speed of whole system by checking the capabilities of each axis that will displace. If an axis is not capable of reaching the desired federate in a specific displacement interval, then the federate is optimized by looking at its maximum jerk capability. In other words, even if the other axis is capable of reaching the desired federate between two CL points, their speed is also reduced because of the slower axis. Thus, the machining time increases and the efficiency of the operation decreases. However, if the NC Code is generated by analyzing the boundary conditions due to the axis characteristics, the process would be faster and more productive.

The objective of this study is to develop a new algorithm which takes the axis drive characteristics of a multi-axis CNC machine tool as an input and generates a more efficient G-Code with recalculated feedrate values and also lead and tilt angles (Figure 1-3 & Figure 1-4) that can be executed by the CNC machine tool in a shorter time. The new lead and tilt angles are being chosen according to chatter stability, maximum cutting force and maximum acceleration and jerk limits of each axis of the system. For such a purpose, the characteristics of each axis of the CNC machine tool is modelled. The developed model is also integrated to previously developed models about maximum cutting forces and chatter stability limits for multi axis milling operations. At the end of execution of the algorithm, the output is a G-Code with recalculated and optimized lead and tilt angles. Simulation and test results that prove the improvements will be demonstrated in the further chapters of the thesis.

1.4 Outline of the Thesis

The main part of the thesis will start with a general overview of the state of the art in feedrate scheduling in machining. In section 2.1 a general introduction to feedrate scheduling will be done. Section 2.2 and section 2.3 discusses feed drive systems and feed generation topics. Different feedrate scheduling algorithms can be found in section 2.4. In section 2.5, a general information about the lead and tilt angle effects on the machining operation will be discussed. Finally, in the final section of Chapter 2, the research gap and motivation of this thesis will be represented.

Chapter 3 will be mainly about acceleration and jerk limitations on CNC machine tool axes. In section 3.3, the test setups and experimental results will be represented. A model developed to predict machining duration will be discussed in section 3.4.

Chapter 4 will continue with feedrate scheduling for multi-axis machining operations. The main problem and starting point topic discussed in section 4.2. Also 7 different cases available for feedrate scheduling will be represented in section 4.2 too. Solution methodology for the problem which mainly uses Dijkstra's algorithm can be found in section 4.3.1. Experimental results and simulation verifications which are about the optimization algorithm will be presented in Chapter 5.

Finally, Chapter 6 will try to summarize the study and give an outlook to the potential of future research works.

2 CHAPTER 2 – LITERATURE REVIEW

2.1 Overview

This chapter is organized for reviewing the state of the art in the field of feedrate scheduling and process optimization in both multi-axis machining and robotics applications. Also as another field, lead and tilt angle effects on 5-axis machining operations, which is one of the concerned topics of the study in this thesis, will be reviewed in this chapter too. The main aim of the literature review in this thesis is to present the state of the art techniques in these fields to prepare the reader for understanding the novelty of this study easily.

The constant feedrate value in the G Code that is produced by CAM software is determined by engineers by looking at several parameters such as material properties of the workpiece, tool specifications and geometrical requirements. The absence in this method is about the feedrate's constancy. Even for a very simple machining operation, due to the variability of geometrical and physical situations of the tool and workpiece, and also the capability of the CNC machine tool, there may occur variable cutting conditions. These variable situations allow different feedrate values along the tool path. Feedrate scheduling can be seen as an answer for this problem, which readjusts the feedrate according to the boundary conditions and tries to make the process more efficient.

As the demand for high speed machining in automotive, aerospace and die and mold industries is grown, the efficiency and quality of the process became a crucial topic in both machining and robotic fields. Feedrate scheduling techniques are being developed for machining time and production cost minimization. To obtain a better efficiency in terms of time consumption and a better final part quality many studies are done in feedrate scheduling and machining parameter optimization.

2.2 General Information about Feed Generation

CNC machine tools processor generate the feed and interpolates the motion throughout the tool path. All of the variables such as position (s), velocity (v), acceleration (a) and jerk (j) are being controlled by the processor instantaneously. These values have to be within some boundary conditions to protect structural unity of the CNC machine tool and also avoid excitation of the natural modes of the system. If the structural modes are excited, the CNC machine tool may start to vibrate at one of its own natural frequencies which is an undesirable situation. If this occurs during cutting process, it is known as chatter vibration which decreases the final part surface quality and also the lifespan of the crucial components in the CNC machine tool. To avoid this phenomenon Erkorkmaz and Altintas [8] proposed the generation of jerk limited feedrate profile. There are two more challenges for the CNC processor while generating a successful feed profile. First of all, the desired feedrate for a machining operation has to be reached if its requirements are within the maximum velocity, acceleration and jerk boundaries. For instance, if the desired velocity change requires a longer displacement than the toolpath displacement, then the execution of that velocity change became unfeasible. The desired feedrate has to be decreased to feasible threshold so that it is achievable. This provides continuous and gradual changes in the feedrate modulation.

Secondly the feedrate modulation must be continuous and smooth through the toolpath. Erkorkmaz and Altintas's [8] proposed method generates feed by starting with piecewise jerk profiles. When the jerk profile is piecewise, the acceleration became trapezoidal thus the feedrate profile has an S-shape with transient changes. It became nearly impossible to excite the structure with a smooth S-shape feed profile. If the desired motion provides these conditions, kinematical and structural compatibility is obtained and the motion can be executed.

In this study, the modifications on the G Code are done with this framework too. As the feedrate is being generated by defining the piecewise jerk profiles, the feedrate is being formed in a smooth s-shape profile. The algorithm guarantees that the motions of each axis are continuous and also within the boundary limits of acceleration and jerk capabilities.

2.3 Feedrate Optimization and Scheduling

It can be said that there are many ways to increase the efficiency of the machining operations, some of which are (1) Feedrate Scheduling Based on Cutting Forces or MRR (Material Removal Rate), (2) Feedrate Scheduling Based on CNC Drive Limitations and (3) Toolpath Optimization Algorithms. All of these techniques have similar objectives which are to reduce machining duration, increase the final part quality and improve the efficiency of the operation.

One of the first studies about feedrate scheduling is started with a technique which tries to keep MRR (Material Removal Rate) constant through the machining operation. Takata et al. [23] proposed a geometrical algorithm which simulates the machining operation geometrically and after that, a physical justification of the proposed model. First of all, in the study, a maximum cutting force is found from tool – workpiece couple and the optimum depth of cut information is calculated. In the geometrical simulation, a technique called ‘Z-Buffer’ is used for extracting a 3D map of the tool and the workpiece. Every step of the algorithm is based on this method which divides the workpiece and the tool into infinitesimal cubes. When the tool and the workpiece is intersecting at a CL (Cutter Location) point, the cubes from the workpieces intersection location is being removed. The algorithm tries to keep the number of cubes being removed at a time and recalculated the required feedrate for each location.

The main aim for the study of Takata et al. [23] is to keep the cutting forces that are being applied on the tool stable at a range and keeping the tool deflection stable. As the cutting forces kept stable, the deflection range is minimized too. This affected the final part’s dimensional quality while speeding up the machining operation. For instance, if the tool – workpiece engagement is small at a certain CL point compared to other CL points, the feedrate value is increased to keep MRR constant. As a result, the machining duration is minimized and approved by experimental justification. However, the study of Takata et al. does not deal with CNC machine tools axis drive capabilities such as their maximum acceleration and jerk limits.

Another case study done by Jerard et al. [17] about toolpath feedrate optimization by the means of maximum cutting forces. In the paper the maximum cutting forces and machining times are compared with those achieved using constant feedrate of traditional machining and the methods of optimization techniques. During the study a mold for a bottle is machined with a 3-axis CNC machine tool. In the traditional method a table based approach is used in which the proper surface cutting speed is found, and the spindle speed required to achieve that specific cutting speed is calculated for a given tool diameter as can be seen in Equation (2.1) where N is the spindle speed, V is the cutting velocity and D is the tool diameter.

$$N = \frac{V}{\pi D} \tag{2.1}$$

After calculating the spindle speed, the proper feed per tooth value is found by looking at the related table to calculate feed value by Equation (2.2) where f_t is feed per tooth value and n_t is the number of teeth on the tool.

$$f = f_t \, n_t \, N \tag{2.2}$$

However, the feedrate optimization procedure is different than the table based traditional approach. Some previously known models [12 - 15] are used to calculate cutting forces in each direction for each tool path location. When machining a sculptured surface, the machined geometry constantly changes and vary chip removal rates can result in large cutting force variations. As knowing the maximum allowed cutting force for minimum tool deflection, the feedrate value is reorganized to maintain a constant force. The results are pretty significant where the roughing operation duration is decreased by 14 percent and finishing duration reduced by 13 percent. Another improvement was done in maximum cutting forces that are reduced by 70 percent that can be seen in Figure 2-1. The study shows clearly the productivity potential of feedrate scheduling techniques.

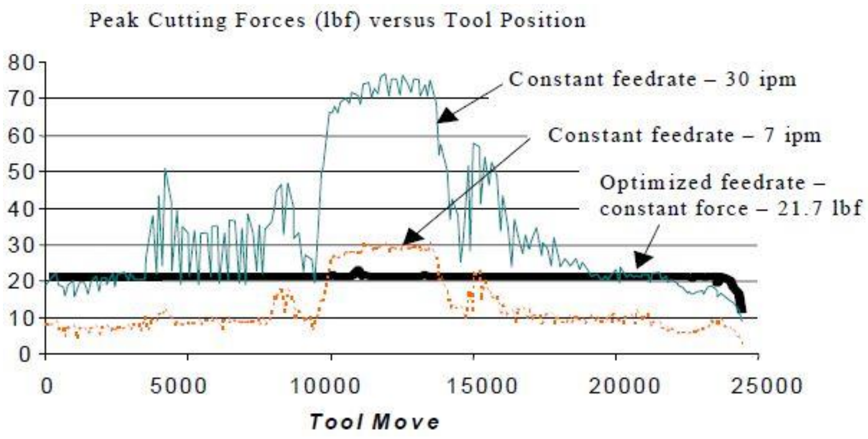

Figure 2-1: Simulated Peak Cutting Forces [17]

Volumetric feedrate scheduling and force based feedrate scheduling techniques are compared by Erdim et al. [7]. Their new mechanistic approach is compared with the basic MRR method theoretically and experimentally for a ball end milling operation. Their approach is setting the feedrate values at each interval on the toolpath by looking at the previously estimated cutting forces and adjusting it considering constant cutting forces.

The study showed that MRR based feedrate scheduling technique generally allows higher feedrate values where force based strategy is more conservative. Due to the higher feedrate values given by MRR technique, cutting forces increased significantly that can damage the part quality or interfere the machining operation.

This phenomenon can be explained by the Figure 2-2. There are 2 different cutting cases in the figure. Both have the same Material Removal Rate which is 1.2 lt/min. However, when the graphs of power consumption by the spindle is investigated, the average power consumption is higher for the Case 2. This proves the MRR based feedrate scheduling approach is not reliable as force based approach.

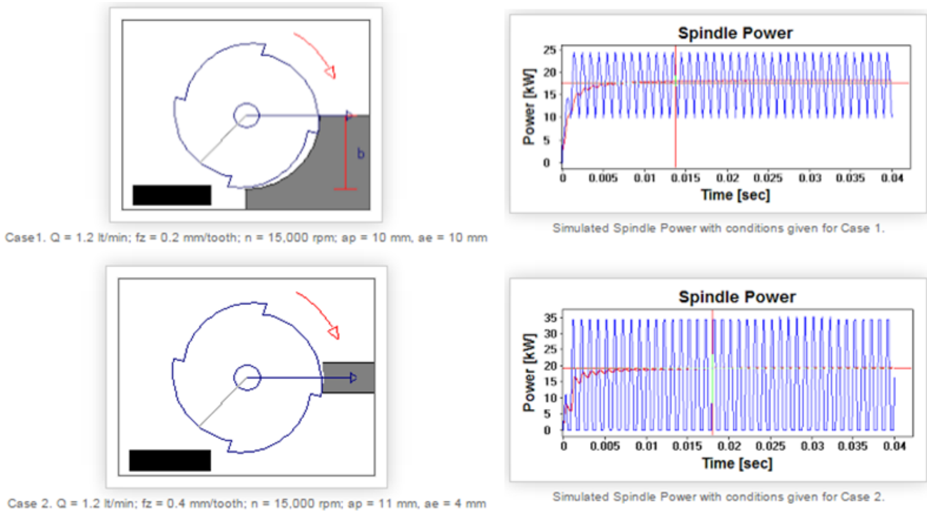

Figure 2-2: MRR – Spindle Power Requirements [27]

Since the volumetric approach rely on geometrical calculations but not on the mechanistic characteristics of the machining operation, it became harder to keep the cutting forces at a certain interval by limiting the MRR. The study introduced a new uncut chip thickness model to the previously known cutting force model and the resultant forces can be kept in the threshold value. The production times are reduced 45-65% during the tests.

The machining process is not affected by only the mechanical characteristics of the operation but also CNC machine tool's own specifications. Tounsi et al. [25] studied the identification of acceleration and deceleration profiles of feed drive systems. Feedrate generation and trajectory planning generally disregarded the limitations from the feed drive systems such as jerk and acceleration. As a result, the prediction of feedrate before the operation may be poor in such cases. This affects the machined part quality and also the operation. Identification of acceleration/deceleration capabilities of the CNC machine tool's axis is crucial in order to achieve desired feedrate at a specific tool location. After the identification of characteristics, Altintas and Erkorkmaz [9] developed a feedrate optimization technique for minimizing the cycle time in machining toolpaths. The maximum jerk, acceleration and velocity values for each axis are taken into consideration throughout the motion to guarantee smooth operation of servo drive without saturation in the publications [3], [9] and [19]. Also minimal tracking error for toolpath is achieved. The continuity of feedrate is obtained by the model developed without any violation of axis jerk, acceleration or torque limits. The proposed algorithm is proved by the tests that it can reduce machining time up to 30 percent.

The generation of proper feedrate and toolpath by looking at the CNC machine tool dynamic characteristics is studied by Dong et al. [6]. They introduced a new acceleration continuation procedure to feedrate scheduling algorithm to remove the discontinuities in the profile and also to address jerk constraints of the CNC machine tool. The proposed algorithm looks at various state dependent constraints such as velocity, acceleration, jerk and position. The method provides viable feedrate solutions in critical points such as crucial curves on the trajectory. In some cases, the jerky motion commands lead to CNC machine tool excitation, thus poor final part quality and also wear in transmission and bearing elements of the axis. By removing the discontinuities in the acceleration profile by looking at the jerk and maximum torque constraints, a time optimal operation is obtained for a 3-axis Cartesian machine. Timar and Farouki [24] conducted another study on 3-axis Cartesian CNC machines for finding time optimal feedrate solutions by taking speed dependent axis acceleration bounds into consideration.

Some studies on 5-axis CNC machine tools are also conducted for feedrate scheduling techniques by looking at its drive constraints. Sencer et al. [22] proposed an algorithm for minimizing machining time on a 3-axis operation of contour machining for sculptured surfaces. The variation of feedrate along the 3-axis toolpath is defined in a cubic B-spline form. The main aim was to minimize tracking error by generating continuous and smooth operation of servo drives along the toolpath by considering velocity, acceleration, jerk and torque limits. If the torque limits are not surpassed, the violation of the saturation limits of the servo drives will be avoided. This will provide a better accuracy and performance from the CNC machine tool as the control dynamics is used in the linear region. To reduce the violation of CNC machine tool drive limitations, Heng and Erkorkmaz [16] studied the fluctuations in the feedrate throughout a multi-axis toolpath. Their proposition is that there are two challenges for realizing a multi-axis machining operation successfully, which are minimizing the feedrate fluctuations and having the feedrate changes continuously without any incoherence. A feed correction polynomial concept is applied to toolpaths to minimize unwanted or unfeasible feedrate changes. A feedrate modulation strategy is applied which relies on trapezoidal acceleration profile.

The jerk profile of a trapezoidal acceleration is continuous also. This leads to smooth changes in velocity and consequently a better part quality.

In another study done by Erkorkmaz et al. [10] the force based approach is merged with CNC machine tool's drive limitations while extracting the new feedrate profile. The algorithm starts with generating the CL data from the CAM model with commercial software. The tool – workpiece engagement conditions are found with CAM model and CL point data. With the data of engagement, the resultant cutting force can be calculated. The simulation of toolpath is conducted with two different feedrate values and the linear relationship with feedrate and cutting force is obtained for each CL point. This step made the determination of local feed limit possible which changes with the individual cutter locations. Locational feedrate limits are extracted and compared with the original G Code generated with traditional techniques. If there is a significant gap that CNC machine tool is not using its potential, the feedrate value can be increased. After the scanning of each CL point feedrate values, the feedrate is increased where it is necessary. After the calculation of optimized feedrate, the next stage which is about CNC machine tool's drive limits starts. In this stage the newly generated, optimized feedrate profile is examined whether the axis is capable of reaching those velocity values or not. If there is a velocity change that exceeds jerk and acceleration limitations of the machine, the feedrate is decreased. This two stage algorithm achieve approximately 16% less machining time cost while guaranteeing that the CNC machine tool drive limits are not exceeded.

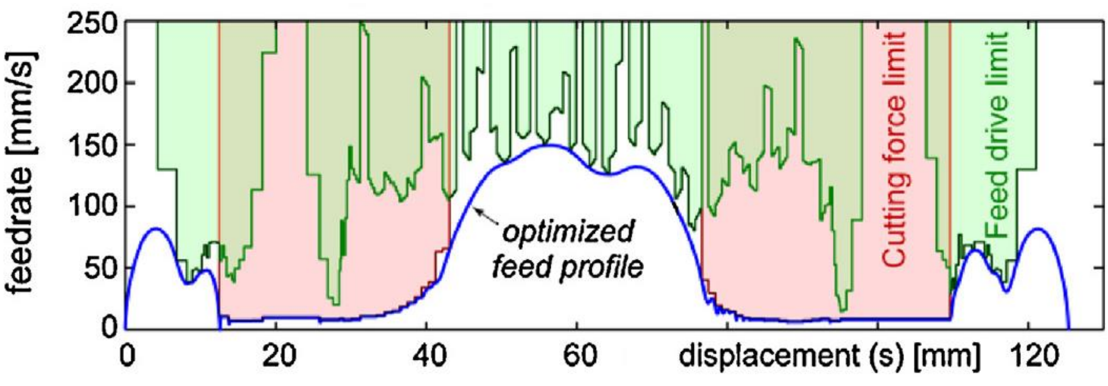

Figure 2-3: Optimized Feed Profile According to Force & Drive Limits [10]

The Figure 2-3 helps to visualize the algorithm. During the displacement of tool along the path, there may exist several constraints. For instance, while green areas representing feed drive limitations, the red areas are for mechanical limits such as cutting forces. So the feed profile should be extracted such that it will not intersect with those areas. At some locations, the main constraint is the cutting forces, and at some other the CNC machine tools drive system limits the operation. After generating the appropriate feedrate profile, the machining duration decreased while drives are used within their limits. During the research done for this thesis a similar approach will be used. However, the main difference will be that the proposed algorithm in this thesis deals with 5-axis operations, especially rotary axis motions and limits.

Another technique for increasing the efficiency of the machining operation deals with toolpath optimization. Many studies in this topic concentrates on cornering stages where the jerk and acceleration requirements from the CNC machine tool increases. Erkorkmaz and Altintas [8] & [9] proposed a new trajectory generation algorithm that generates continuous profiles for each position, velocity and acceleration variables. The feedrate fluctuation is also eliminated which may occur due to parameterization errors. Another toolpath smoothing algorithm is used by Beudaert et al. [4], Lee et al. [18] and Ernesto and Farouki [11]. Their main focus is to smooth the tool path by avoiding sharp turns or commands that require high jerk. The proposed algorithm smoothens the toolpath without violating the chord length error tolerance which is the perpendicular distance between the commanded toolpath and realized toolpath at each CL point. When the tool path is smoothened, the motions that require high jerk values, high deceleration or acceleration motions will be avoided. When there is no need for high deceleration or acceleration rate, the operation became more feasible so the machining duration is minimized significantly.

The study in this thesis is using some of the techniques used in feedrate scheduling with toolpath optimization on some level. The original toolpath is not changed in the algorithm when the CC (Cutter Contact) points are taken into consideration. However, while CC points are not changed, it is necessary to modify CL points when the tool orientation vector is modified.

2.4 Lead & Tilt Angle Effects on 5-Axis Machining

The lead and tilt angles provided by 4^{th} and 5^{th} axis on the CNC machine tool has significant effects on the machining operation dynamics as well as the final part quality. Ozturk et al. [20] investigated the effects of tool tip contact on the surface finish quality. Their investigation extended to the effects of lead and tilt angles on the cutting forces, torque requirements, form errors and stability. The drastic variation of dynamics and mechanics of cutting operation with the lead and tilt angle changes is verified. It is proven that with some lead and tilt angle combinations, cutting forces and stability limits can be quite different.

It can be said that 4^{th} and 5^{th} axes should not be used only for geometrical constraints but also for a better and more efficient machining operation. It can be used for avoiding tool tip contact which may result in ploughing indentation on the machined surface causing poor surface finish. Additionally, the with the increased tilt angles the scallop height can be minimized so step over values can be increased [20]. This results in higher productivity and efficiency in multi-axis milling operations. Also the cutting forces may be modified by changing the lead and tilt angles [21]. For instance, during roughing operation it is shown that the usage of the lower side of the tool generates lower cutting forces thus requires lower cutting torque and power. At last but not least, by changing the lead and tilt angles, the stability of the operation can be modified. In the study of Ozturk et al. [20] it is proven that some lead and tilt angle combinations may increase absolute stability limit 4 times higher.

The study in this thesis deals with lead and tilt angle intervals in multi-axis machining operations. The proposed algorithm focuses mainly on roughing operations and selects lead and tilt angle combinations from the feasible region which reduces the machining duration.

As mentioned earlier, it is possible to machine the same sculptured surface with a multi-axis machining center with different tool postures. [1] Lead and tilt angles can be readjusted to minimize cutting forces while increasing final part quality. However, there is another constraint while adjusting the lead and tilt angles for a multi-axis machining operation. A feasible lead and tilt angle threshold is defined for a stable machining operation without any chatter vibration and the algorithm developed in this study determines a specific the lead and tilt angle value for each CL point which decreases machining time without any jerky motions.

During a 5-axis machining tool path generation, the tool axis is generally selected according to the geometrical constraints. However, the effects of the tool axis are also significant on final part quality and also CNC machine tool motion. For the first time in the literature, the study of this thesis, proposes an algorithm which readjusts the lead and tilt angles of the tool by taking maximum allowable cutting forces, stability, machining duration and machine tool motion capabilities into consideration.

2.5 Motivation

The objective of this study is to make the multi-axis machining operations more efficient. By the usage of a novel algorithm, the technique in this study outputs a better metal cutting process with lower average cutting forces and a better surface finish. In multi-axis machining operations, the interpolation of the axis plays a significant role in obtaining the final part geometry. The algorithm checks whether the standard interpolation is efficient or not. If it is not efficient, in other words if there is an axis which reduces the speed of the process, the algorithm selects another cutting geometry which will speed up the process and also gives a better surface finish. This will be done by checking the maximum capabilities of each axis drive and also the cutting process dynamics. For instance, in 5-axis machining operations, the lead and tilt angles are obtained by 2 rotary axis of the CNC machine tool. The same final part geometry could be obtained by different tool postures too. So the process may be optimized by choosing the best lead and tilt angles at each cutter location by checking the axis drive capabilities such as maximum jerk and acceleration limits. The feedrate and tool posture is optimized accordingly which gives a better surface finish in a shorter machining duration.

Numerous studies are conducted on feedrate scheduling based on material removal rate, resultant cutting forces and CNC machine tools drive limitations. However, previous studies did not approach process feedrate optimization by looking at the effects of machine tool axis drive capabilities and tool postures. Numerous CNC axis drive characterization tests are conducted during the study which outputs the axis drive limits of the machine tool and real machining durations are estimated accordingly. All axis capabilities such as maximum velocity, acceleration and jerk are captured with the tests. That data will later be used in choosing the optimum axis motions to speed up the system and obtain a better surface finish.

3 CHAPTER 3 – ACCELERATION AND JERK LIMITATIONS

3.1 Introduction

In this chapter, the tests conducted for identifying the CNC machine tool's drive limits will be represented. The test is required for detecting the limited capacity of the system which will be later used as an input for the simulation models. During the tests, an alternative approach is done for the investigation of CNC machine tool's acceleration/deceleration capabilities can by observing its feed-drive's jerk limitations. A developed model to estimate machining duration which can be extracted from a given G Code will be presented in the further sections of this chapter. The feed-drive's jerk limitation and a G Code is given to the model which then calculated the cycle time.

3.2 Feedrate Profiles

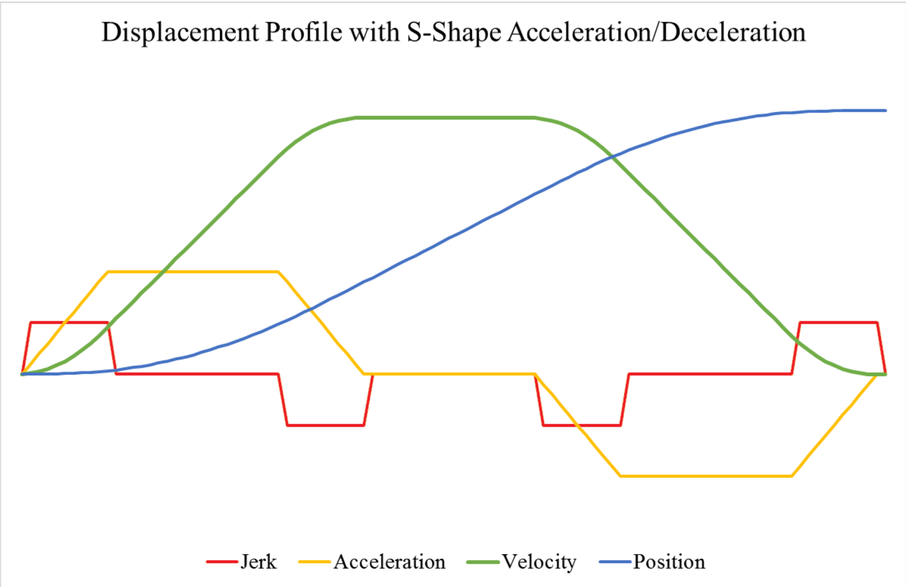

Figure 3-1: Displacement Profile with S-Shape Acceleration/Deceleration

The type of motion represented in Figure 3-1 has an S-Shape acceleration and deceleration intervals. The steepness of the acceleration and deceleration phases are defined by jerk value which is its derivative. The non-zero flat profiles in the jerk graph is known as Jerk Percent. Jerk percent is the percentage of time where the jerk is constant and non-zero. This percentage defines how much the acceleration and deceleration phases are curved. If there is a duration between the zero and non-zero phases of the acceleration curve, the jerk percent became non-zero as can be seen in Figure 3-1. In other words, when the jerk profile is examined, there are some interval at which the jerk is non-zero and constant. This interval makes the jerk percent different than 0. When the jerk percent is 0, it can be said that jerk profile consists of step inputs and zeros. There are no continuous non-zero phases in the jerk profile. This makes the motion has a trapezoidal profile as can be seen in Figure 3-2. The difference can easily be seen by comparing the profiles in Figure 3-1 & Figure 3-2.

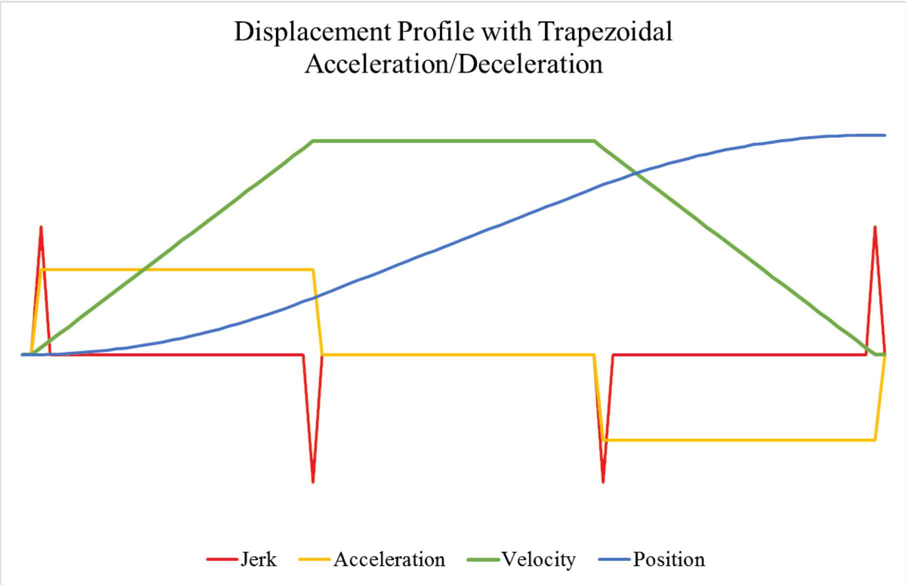

Figure 3-2: Displacement Profile with Trapezoidal Acceleration/Deceleration

If the feed-drive reaches its jerk limit during a motion, the jerk percentage will be a non-zero value. It means that the jerk limit reached its maximum value and the feed drive is saturated. However, if the feed-drive does not reach its jerk limit, the jerk profile will not have the flat interval resulting in a peak shape. This happens when the displacement in not sufficient for the axis drive to reach the commanded feedrate or it can be the acceleration limitation which limits the jerk profile. This is when the Feed-drive control steps in. The control algorithm starts to limit the jerk value without reaching the maximum value to prevent the overshoot in the tool path.

For instance, if the reachable velocity in a specified displacement interval is smaller than the commanded one, the Feed-drive control reduces the commanded value to the maximum reachable one. This will prevent the CNC machine tool structure to stay in the geometrical tolerances without any overshoot.

3.3 Experimental Setups and Results

Two different systems are used for measuring CNC machine tool axis maximum jerk, acceleration and velocity. By conducting the experiments with two different setups, the accuracy of the results could be approved. Also, as one of the measurement sensors measuring range is limited, another system had to be used for long range displacement measurements. The main goal was to compare the given feedrate commands with the actual feedrate values of the CNC machine tool. Later the data will be used in MATLAB machining simulations.

3.3.1 Laser Displacement Sensor Test Setup

In the first setup that is prepared for short displacement measurements, a Keyence LK-G5000 series laser displacement sensor is used (Figure 3-3). The variant that is used in tests has a repeatability of 0.005μ and an accuracy of ±0.02% which are the highest values in its class. As the sampling rate of the sensor is 392 kHz any of the jerk or acceleration fluctuations can be captured during the tests.

Figure 3-3: Keyence LK-G5000 Series Laser Displacement Sensors

The laser sensor test setup consists of 2 different configurations. In the first configuration, linear axis characteristics are measured and in the second configuration, rotary axis characteristics are investigated. For the first configuration that can be seen in Figure 3-4, the laser sensor is stationary on the rotary table. A reflective flat plate is placed on the spindle. As the spindle has 3 degrees of freedom which are on X, Y and Z axis, the test setup is configured differently for each of the axes.

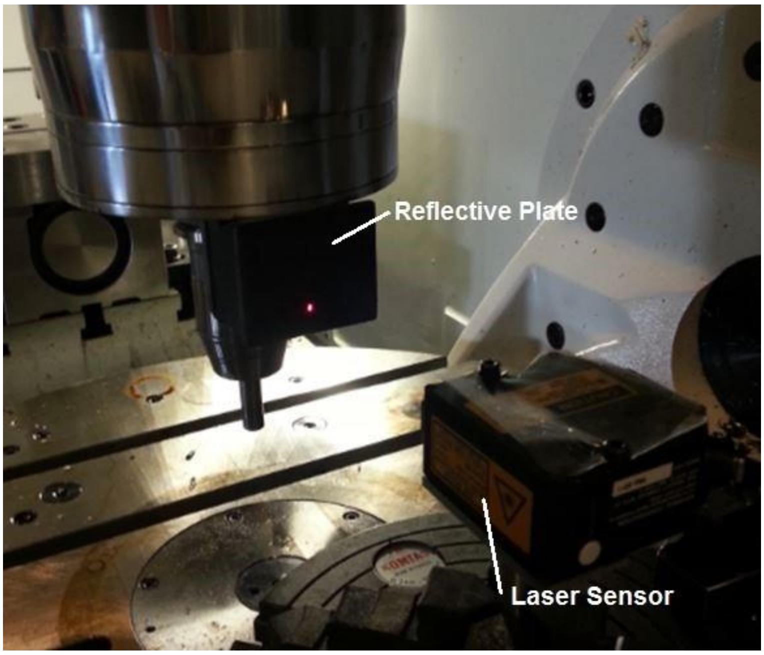

Figure 3-4: Laser Displacement Sensor Test Setup for Linear Axis Measurements

Keyence LK-G5000 series laser sensors have a measurement range of 5mm. During the tests, each of the linear axes are commanded to displace 5 mm with various feedrate values. The feedrate values started from 100 mm/min and increased to 7000 mm/min which will be presented later in this chapter. At each test, the measurements are captured with NI LabVIEW 2013 software and the data of jerk, acceleration, velocity and position is transferred to Microsoft Office Excel 2013 for analysis as can be seen in Figure 3-5.

The graphical interpretation and calculation of jerk, acceleration, velocity and position data was also done with NI LabVIEW 2013 that can be found in Figure 3-6 and Figure 3-7.

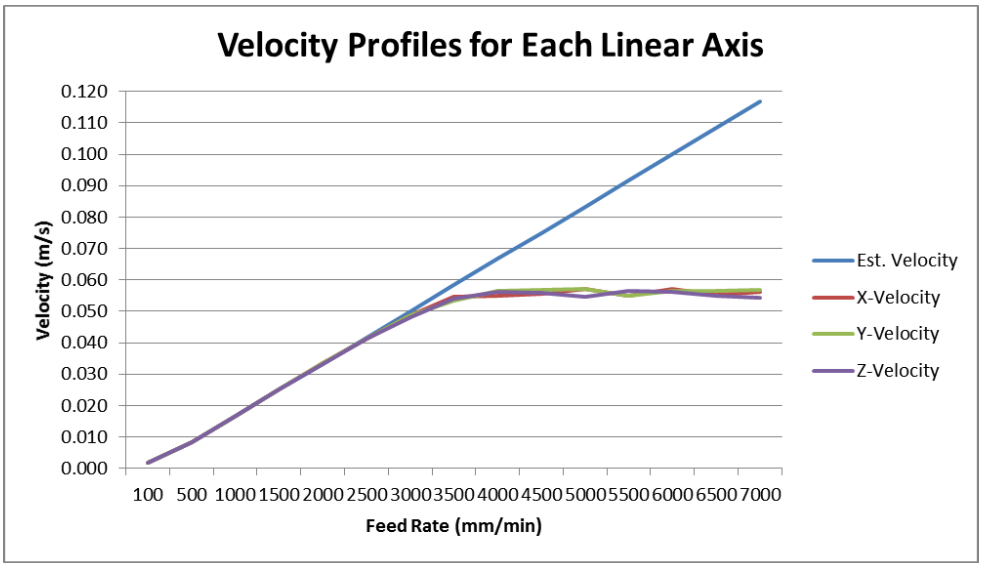

Figure 3-5: Velocity Profiles for Each Linear Axis.

The Figure 3-5 represents the behavior of all 3 linear axis of the CNC machine tool. The feedrate values which are in the X-axis of the graph are the input (commanded) values for CNC machine tool. Y-axis shows the maximum velocity that the axis reached in reality. However, as the capacity of the feed drives are not sufficient and it cannot reach the commanded values after a certain point.

The tests started with 100 mm/min feedrate input. When the maximum axis velocity is measured with laser displacement sensor, it is observed that the axis reached the commanded velocity in the first test. As the first feedrate input are reachable by the CNC machine tool's feed drive system, approximately for the first 7 tests, all of the linear axis are capable of reached the desired speed. However, after a certain point, in this case it was 3500 mm/min, the drive systems start to saturate and it starts to cut down the desired feedrate to prevent the overshoot. As the given G Code commands the system to stop at 5 mm after the start up point, to be able to stop at exactly at that point, the CNC drive processor limits the feedrate and it keeps the maximum speed at around 0.060 m/s which is approximately 3600 mm/min.

The observed linear axis characteristics were very similar between X, Y and Z axis. The feed drive system of all the linear axes are saturated around 3600 mm/min whatever the given input was. More detailed data about the laser displacement sensor test can be found in Appendix A: Linear Axis (X – Y – Z) Measurement Data (Velocity – Acceleration – Jerk – Duration).

With Figure 3-6 and Figure 3-7 , which are captured from NI LabVIEW 2013, a comparison can be done between a feedrate that is reachable by CNC feed-drive system and a feedrate that cannot be reachable.

In Figure 3-6, the axis behavior against 500 mm/min feedrate input can be seen. As stated before in this chapter, the movements observed are trapezoidal movements which means that jerk percentage is 0. This can be observed by looking at the figure below too.

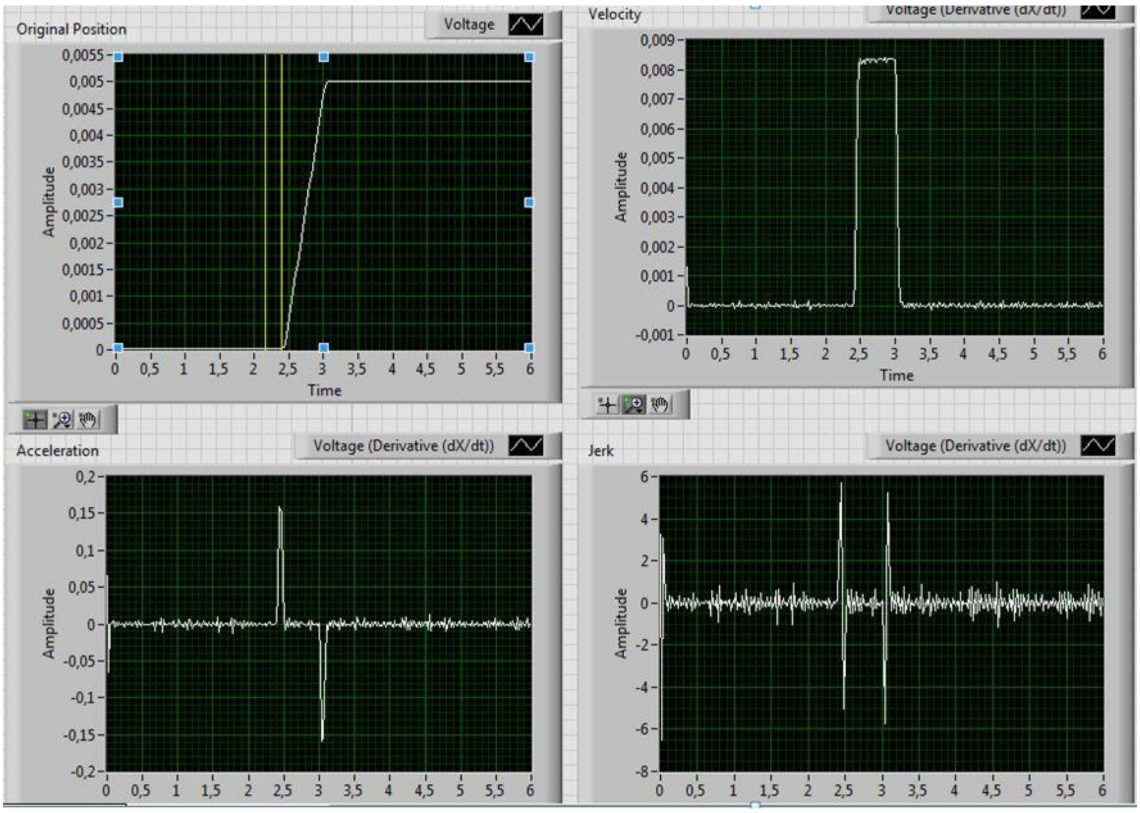

Figure 3-6: Axis Behavior for 500 mm/min Feedrate Input

The top left graph presents the displacement data. It shows that the measurement lasted 6 seconds and at approximately 2.5th second after the measurement was started, the axis started to move and at approximately 3rd second it reached its destination which is 5 mm ahead from the starting point. The top left graph consists of the velocity data during the motion. As can be expected, the velocity is 0 until 2.5th second and it reaches the desired value before 3rd second. The bottom left graph is for visualizing the acceleration data of the motion. At 2.5th second, there is an acceleration peak and at 3rd second there can be seen a deceleration extremity which finishes the motion. The last graph which is at the bottom right of the Figure 3-6, is the jerk graph which shows the changes in the acceleration.

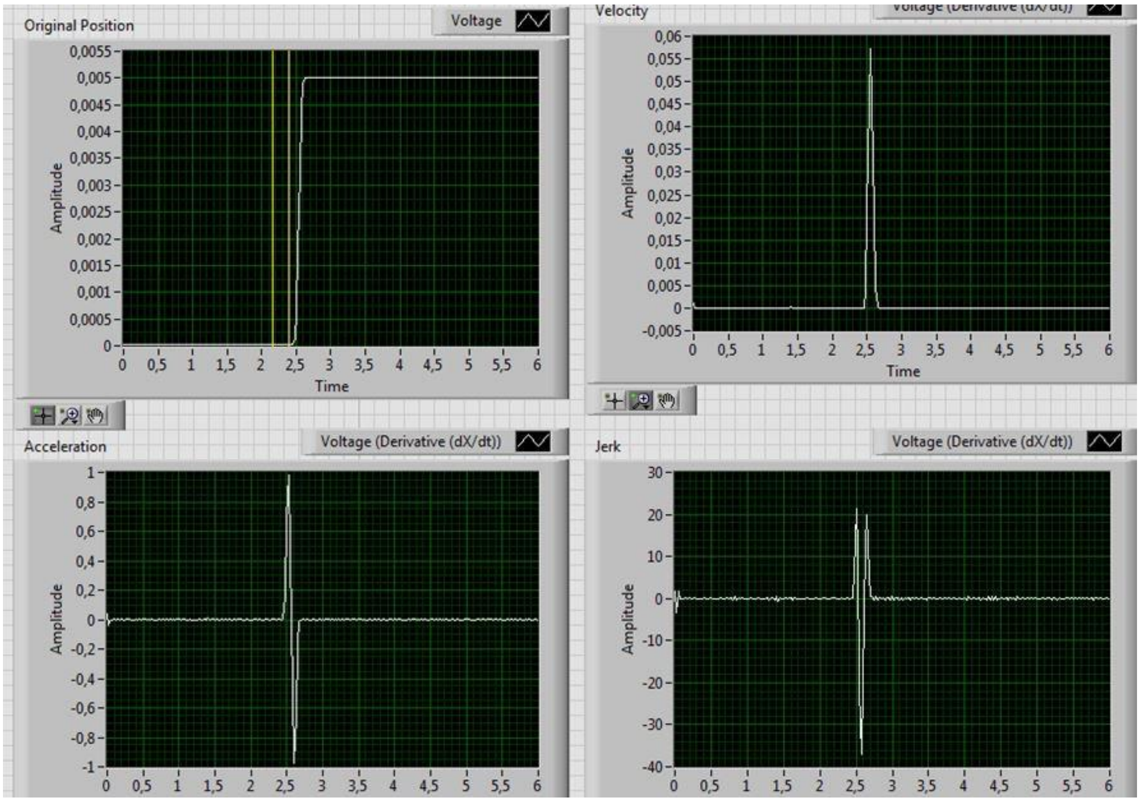

Figure 3-7: Axis Behavior for 6000 mm/min Feedrate Input

As can be seen in the jerk graph in Figure 3-6, there are no top or bottom flat parts but there are only peak points which means that the jerk percentage is 0 for these motions as mentioned in previous parts in the thesis. This peak shape is also valid for acceleration graph too. If the velocity graph is observed, there can be seen a flat interval at the maximum point which means that the desired speed is reached and the axis continued its motion along the path with the commanded feedrate for a while and it decelerated. Therefore, it can be said that the 500 mm/min feedrate command is reached in 5 mm displacement interval.

However, this situation is not valid for 6000 mm/min feedrate command that can be seen in Figure 3-7 in the next page. First of all, the maximum values for jerk and acceleration graphs are larger than the motion with 500 mm/min feedrate. This is for trying to reach the commanded feedrate as expected. However, if the velocity graph is observed, it can be seen that it makes a peak shape and start to decelerate just after its acceleration phase. Also the peak value which is 0.06 m/s (~3600 mm/min) shows that the desired feedrate which is 6000 mm/min cannot be reached. As it is mentioned earlier, this is due to the capability of the CNC feed drive and 5 mm displacement length.

Other than the velocity data, acceleration and jerk data captured with the test setup is analyzed also. The acceleration data in the Figure 3-8 shows that linear axis reaches their maximum acceleration value at approximately 4000 mm/min feedrate command and it is around 1 m/s^2.

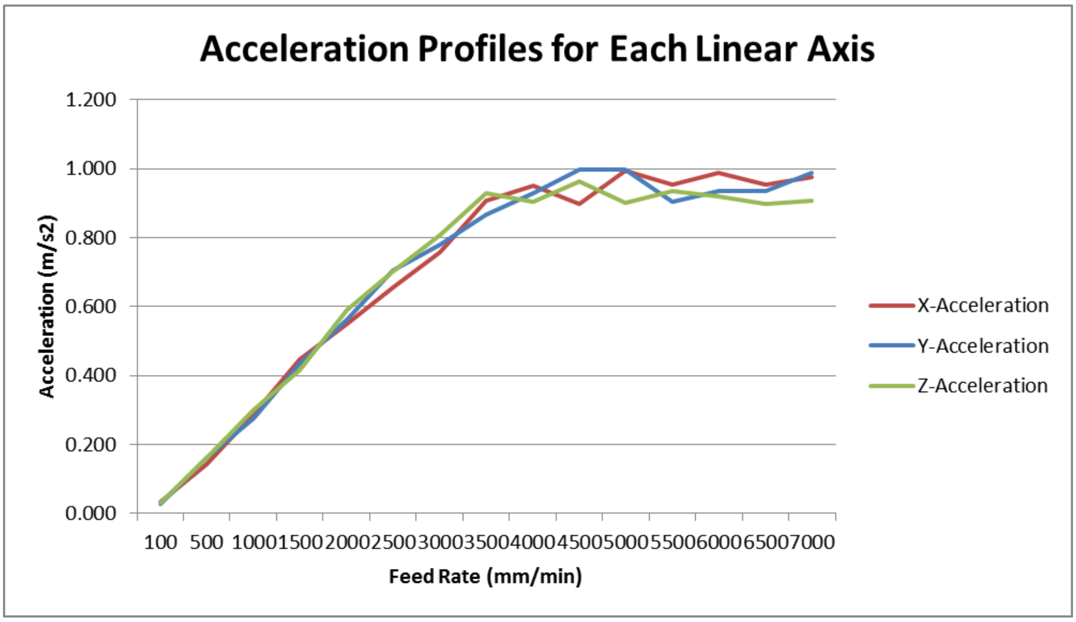

Figure 3-8: Acceleration Profiles for Each Linear Axis

If the jerk vs. commanded feedrate graph is observed as represented in Figure 3-9, the maximum value for jerk is approximately 22 m/s^3 at it is reached around 4000 mm/min commanded feedrate value as acceleration does. At that point, the CNC feed drive actuators become saturated which should be avoided as the system become non-linear after that point and this may lead to instability. This phenomenon can affect the tracking control in a negative way for CNC machine tools. [8]

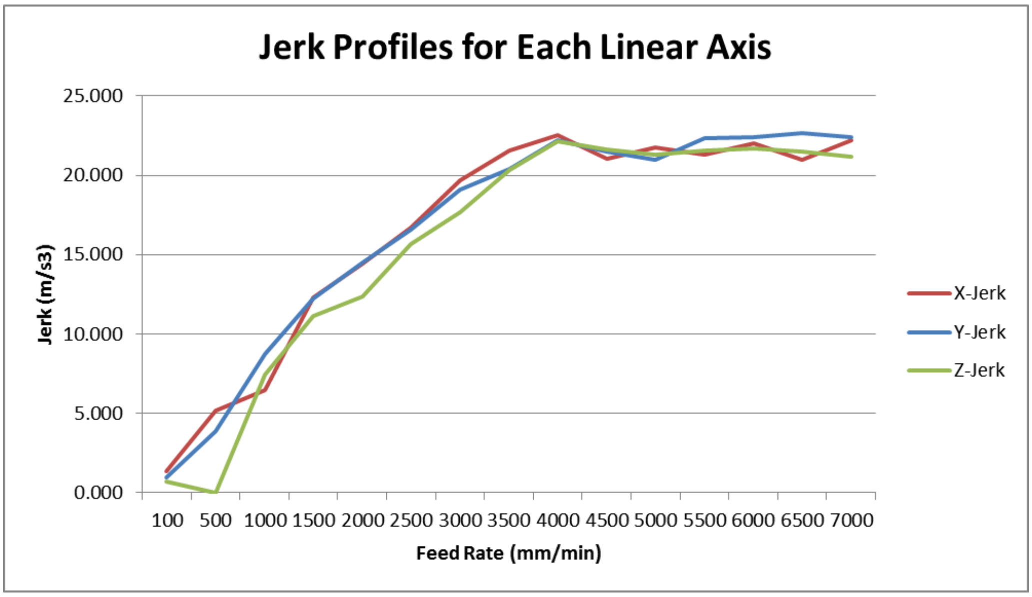

Figure 3-9: Jerk Profiles for Each Linear Axis

The first configuration for laser displacement sensor test setup is used for measuring linear axis characteristics as mentioned earlier. The second configuration with the same measurement tool is used for measuring the 2 rotary axis of the 5-axis CNC machine tool. The laser displacement sensor is mounted on the body of the CNC machine tool and the rotary axis are moved successively. The B and C axis of the system are commanded to move 1^{o} for different feedrate values and the measurement data is captured with the same software and system. The rotary axis test results will be mentioned in a detailed way later in this section.

Some information should be given before passing to the results of the rotary axis measurements about Feedrate Modes G93 and G94. There is an important difference between linear and rotary motion measurement assignment. When the user gives a feedrate value for a linear axis, it is calculated straightforwardly by the CNC processor as the displacement is linear. There is no relative motion for a linear axis, other than a relative motion to CNC machine tools body. In other words, if the user sets the feedrate to 1000 mm/min for a linear axis, the commanded axis tries to travel at 1000 mm/min relative to the body of the CNC machine tool which is stationary.

Figure 3-10: Laser Displacement Sensor Test Setup for Rotary C-Axis Measurements

However, this phenomenon is not valid for rotary axes. As the motion of the rotary axis has a circular form, each individual point of the rotary table has a different linear velocity when it is calculated from circular motion. To solve this problem another feedrate mode is used to measure the circular motion precisely.

The test setup can be seen in Figure 3-10. The reflective plate is situated on the rotary table and the exact distance between the origin and the laser pointer cannot be identified sensitively. So in other words, the G 93 feedrate mode (units per minute feedrate mode) cannot be used for this setup. Let us assume that the X, Y and Z axis are stationary which are on the spindle itself. When the operator inputs a feedrate, the CNC processor calculates the tool tip position and moves the rotary axis accordingly such that the relative speed between tool tip and the rotary table has the linear velocity as the given feedrate. However, it is nearly impossible to locate the tool tip and the laser point at the same precise location.

This is where G 94 feedrate mode (inverse time feedrate mode) steps in. In the inverse time feedrate mode the user inputs the time interval in which the motion has to be completed. F letter means the motion must be completed in one divided by the F number minutes. For example, if the input is 1 the motion has to be completed in 1 minute, if the input is 2, the motion has to be completed in half a minute. By using the inverse feedrate mode, the commanded rotary motion magnitude can be calculated exactly without calculating the tool tip position etc.

Now the test results may be presented. During the rotary axis measurements, feedrate values are converted into angular velocity magnitudes and compared respectively. The rotary axis velocity limits can be observed in Figure 3-11. The inverse feedrate values are converted in to (°/s) units. B – Axis reaches its top speed capacity at around 0.275 °/s and C – Axis maximum velocity stays around 0.225 °/s.

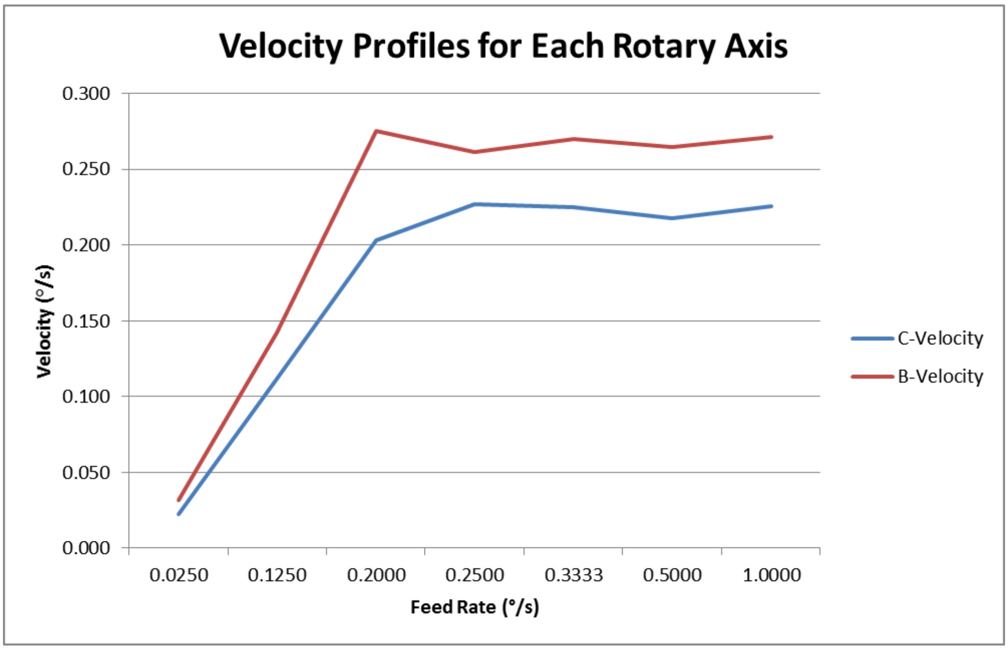

Figure 3-11: Angular Velocity Profiles for Each Rotary Axis

Acceleration and jerk profiles for the rotary axis of the CNC machine tool can be seen in Figure 3-12 and Figure 3-13. When B and C – Axis acceleration profiles are investigated it can be seen that there is no significant difference between each other. However, the C – Axis jerk results are slightly larger than the ones of B – Axis. All of this data is used as an input for the MATLAB simulation for which the results will be presented in the later sections of the thesis.

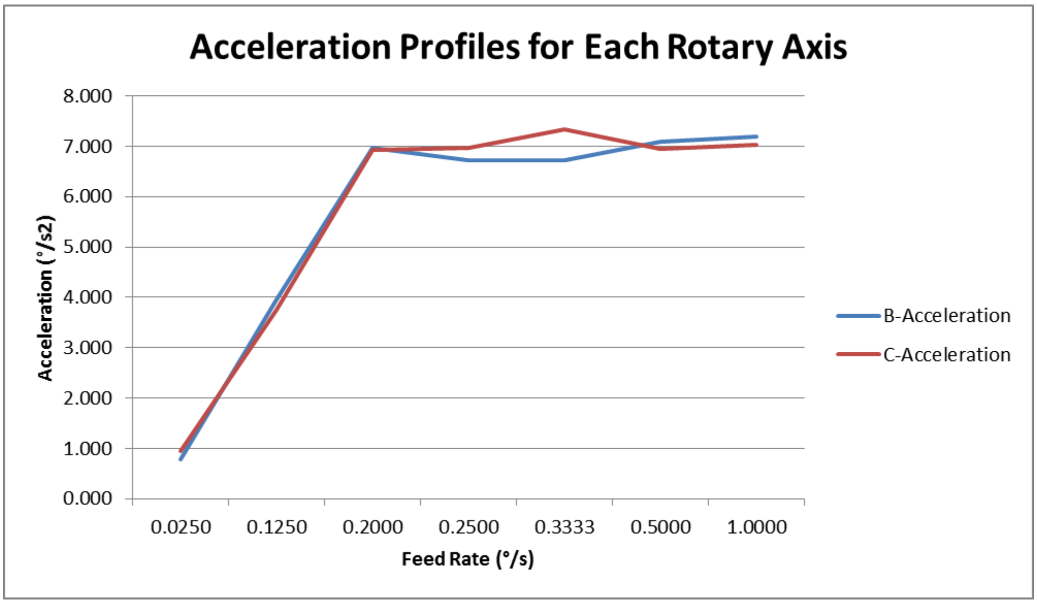

Figure 3-12: Angular Acceleration Profiles for Each Rotary Axis

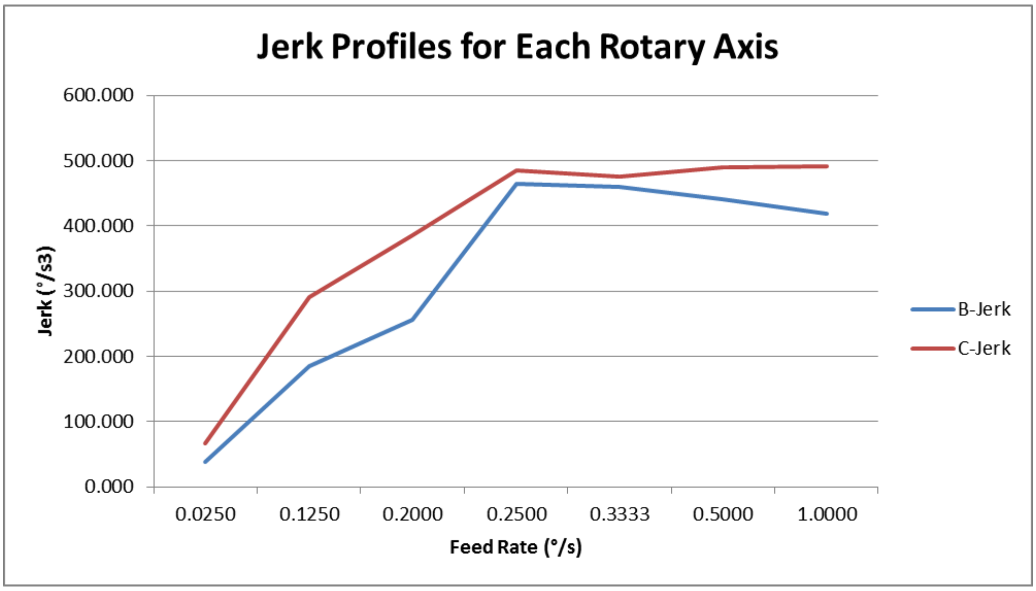

Figure 3-13: Angular Jerk Profiles for Each Rotary Axis

Detailed informative data about rotary axis measurements can be found in Appendix B: Rotary Axis (B – C) Measurement Data (Velocity – Acceleration – Jerk – Duration).

3.3.2 Laser Interferometer Test Setup

In the second measurement setup, a sensor with a longer measurement range is used. It was a Renishaw XL-80 (Figure 3-14) type laser interferometer which has 1 nanometer linear resolution and ±0.5 ppm linear measurement accuracy. It has a lower sampling rate which is 50 kHz compared to Keyence laser displacement sensor's 392 kHz. However, Renishaw interferometers strongest feature against Keyence laser displacement sensor is its linear measurement range which is 80 meters.

Figure 3-14: Renishaw XL-80 Laser Interferometer

With the laser interferometer, the long range movement characteristics of the CNC machine tool could be observed. As the Keyence laser displacement sensor can only work within 5 mm, there is no chance for measurements longer than that value. However, with laser interferometers, tests of 50 mm, 100 mm, 200 mm and 300 mm displacements were done during the study.

The first comparison for the long range tests can be done with same feedrate value and different displacement commands. The acceleration and velocity graphs can be seen in Figure 3-15 and Figure 3-16. The maximum allowed feedrate for the tested CNC machine tool was 48000 mm/min which is the commanded feedrate during 100 mm displacement long range tests.

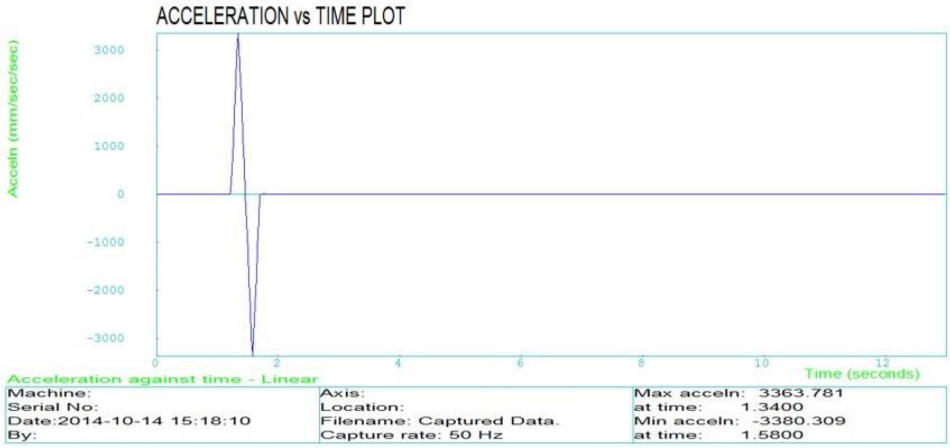

Figure 3-15: Acceleration Profile for 100 mm Displacement (Feedrate = 48000 mm/min)

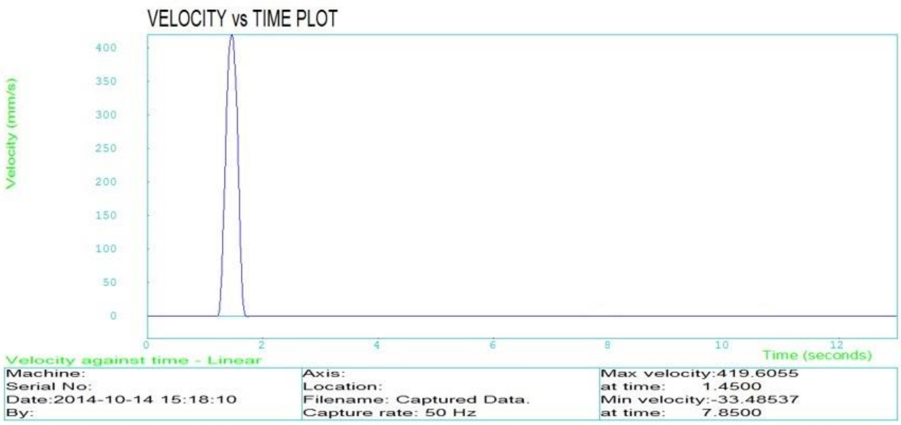

Figure 3-16: Velocity Profile for 100 mm Displacement (Feedrate = 48000 mm/min)

However, as can be observed from the graphs above, the measured axis cannot reach the commanded feedrate and it stays at 420 mm/s (25200 mm/min). The peak shape also tells that the desired speed cannot be reached and the axis starts to decelerate just after its acceleration phase.

In the graphs that can be seen in Figure 3-17 and Figure 3-18 while the commanded feedrate value stays constant at 48000 mm/min, the displacement is increased to 300 mm. The aim was to check whether the long displacement range would allow the axis to reach the maximum feedrate value that is allowed by the CNC. The results show that maximum acceleration is larger than the maximum acceleration measured in 100 mm displacement. Also the velocity profile clearly shows that the desired speed is reached and the velocity profile have a flat interval where the speed stays constant at a maximum value which is 800 mm/sec (48000 mm/min). Various test results captured with laser interferometer can be found in Appendix C: Laser Interferometer Test Results, where the limits of the CNC feed drive can be observer when increasing the feedrate from 1000 mm/min to 4000 mm/min.

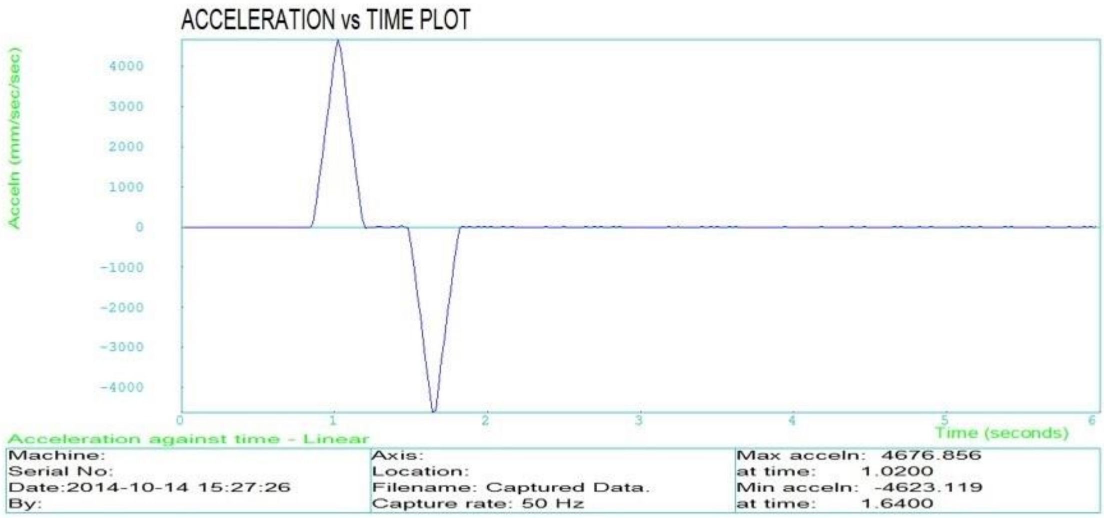

Figure 3-17: Acceleration Profile for 300 mm Displacement (Feedrate = 48000 mm/min)

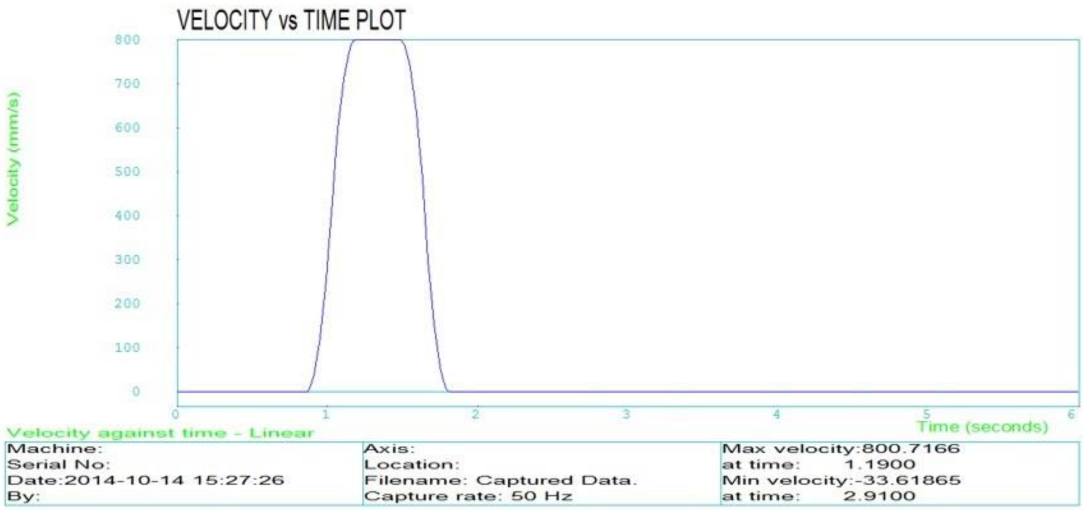

Figure 3-18: Velocity Profile for 300 mm Displacement (Feedrate = 48000 mm/min)

3.4 Simulation Results

All of the data from short range and long range measurement test are observed and a linear relationship between the reachable speed and the displacement command is found. With the linear regression technique reachable speeds for every displacement interval can be estimated. An algorithm developed in MATLAB for the estimation of time required for a given G Code. The jerk and acceleration limitations and also a G Code are given to the algorithm which then estimates the elapsed time for the commanded motion.

For each G01 command the algorithm calculates the displacement, the vector of the motion, the direction of the movement, desired feedrate from each axis and actual feedrate values. Then it calculates the total time required to finish the G Code. Also another output is given which tell the whether the commanded speeds are reached by each individual axis or not.

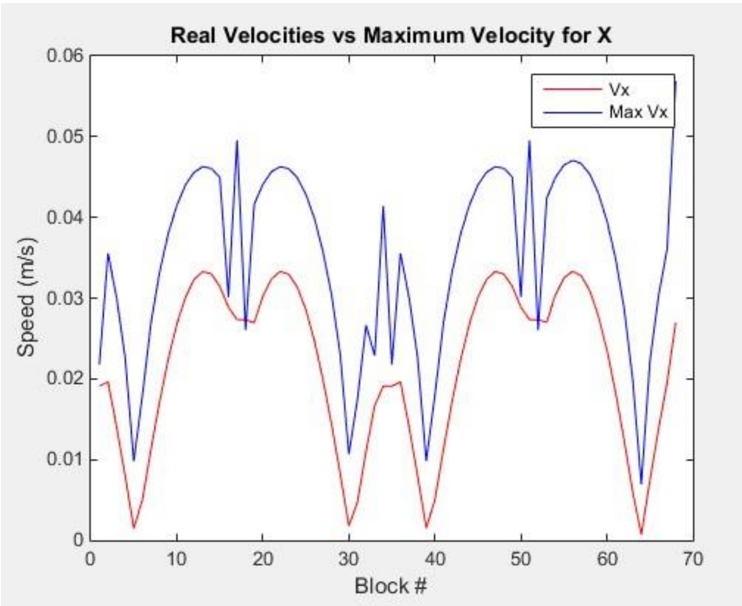

Figure 3-19: MATLAB Simulation Output

An example for the output for a single axis (X Axis) can be seen in Figure 3-19. At each block the maximum reachable feedrate values are calculated and printed on the graph with a blue line. Also the required velocity for providing the commanded feedrate to the used is calculated and printed with a red line on the graph. The graph shows that at Block

#17 and at Block #53 the commanded feedrate cannot be reachable by the CNC machine tool due to the limitations of the X – Axis feed drive. The required duration calculations are done with this method and the error between calculated and measured machining time durations are below 0.5 seconds unbiased of how long the machining duration is. The prediction results can be seen in Figure 3-20 below.

Feed mm/min	Calculated sec	Measured sec	Error sec
500	17.3182	17.84	0.5218
1000	8.7165	9.28	0.5635
1500	5.8747	6.44	0.5653
2000	4.4729	5.19	0.7171
2500	3.6471	3.97	0.3229
3000	3.1094	3.46	0.3506
3500	2.7362	3.43	0.6938
4000	2.4658	2.41	-0.0558
4500	2.2641	2.68	0.4159
5000	2.1103	2.45	0.3397
5500	1.9914	2.34	0.3486
6000	1.8987	2.28	0.3813
6500	1.8262	2.12	0.2938
7000	1.7695	1.68	-0.0895
7500	1.7254	2.29	0.5646

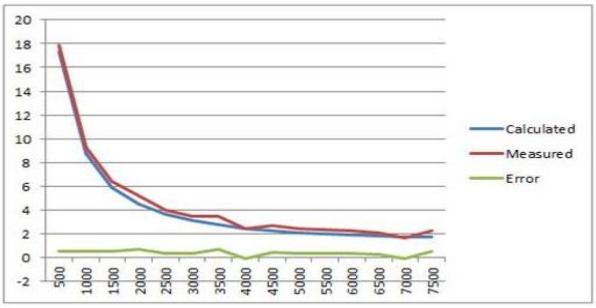

Figure 3-20: Machining Duration Prediction Validation

3.5 Summary

This chapter presented the test measurements done for analyzing the capabilities of a CNC machine tool with different equipment and in different circumstances. The test variables are continuously changed to be able to investigate the characteristics of the CNC machine tool for different situation. Also a MATLAB algorithm is presented which can estimate the total movement duration according to jerk and acceleration limits of the CNC feed drive. During the next chapter, an algorithm will be presented for machining time minimization for a 5-axis machining operation with respect to lead and tilt angle variables and acceleration and jerk constraints.

4 CHAPTER 4 – FEEDRATE SCHEDULING STRATEGIES FOR 5-AXIS MACHINING OPERATIONS

4.1 Introduction

In the machining time optimization literature, majority of the studies tried to optimize the toolpath or modify the feed profile for minimizing cycle time rather than choosing the optimum tool posture with respect to feed drive. During Chapter 4, a novel machining time minimization algorithm with optimum tool axis vector selection with respect to CNC feed drive limitations will be introduced. Before illustrating the main flow chart of the optimization process, a general overview for the problem studied will be presented in 7 different cases to be more understandable. Later in this chapter, the optimization process flowchart and problem solution methodology will be presented.

4.2 Problem and Starting Point

This section will illustrate 7 different cases at feedrate scheduling for machining time optimization from the simplest one through the most complicated one in sequence. The first case will present a 3-axis machining operation with constant feedrate. The second case will be about 3-axis machining operation with force based feedrate scheduling. The third case will add feed drive limitations to 3-axis machining operation with force based feedrate scheduling. The fourth case will be about traditional 5-axis machining operations with constant feedrate. The fifth one represents a 5-axis machining operation with force based feedrate scheduling. In the sixth case, lead and tilt angle optimization will come into play in 5-axis milling operations with respect to stability and force calculations. The final and most important case for this study is seventh case in which the lead and tilt angles will be modified with respect to stability and CNC feed drive limitations.

4.2.1 Case 1: 3-Axis Constant Feedrate

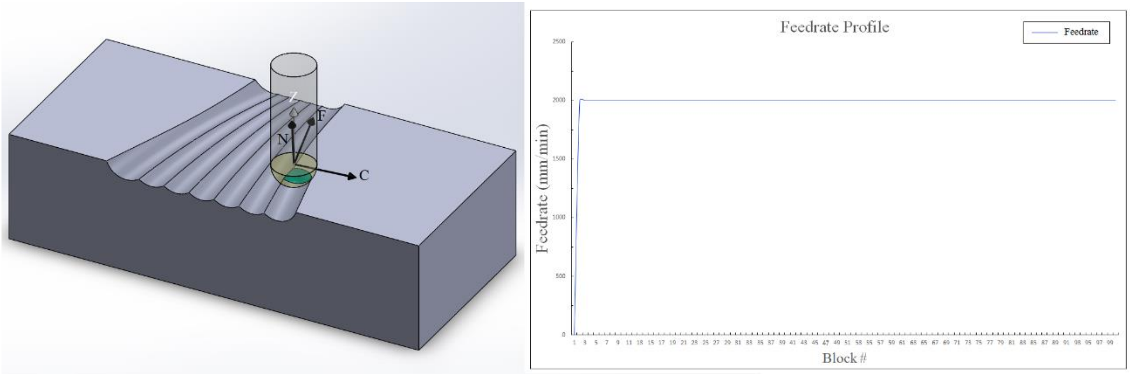

Figure 4-1: 3-Axis Constant Feedrate Machining Illustration

Case 1 can be regarded as the simplest case. However, its simplicity brings miscalculations and also some boundary conditions. The illustration of Case 1 can be seen in Figure 4-1. This can be regarded as one of the simplest machining operation in which only 3 axis interpolation is used in CNC machine tool and the feedrate command is kept constant.

Nevertheless, whatever the commanded feedrate is, the CNC machine tool may not be able to reach that commanded input due to its capabilities. This may occur due to jerk limitations, bulky axis drivetrain or mechanical and controller lags. Therefore, the actual feedrate may differ from the commanded one. This undesirable situation may affect negatively the machining time prediction. Again, it may decrease the accuracy of the CNC machine tools tracking control [8].

Also, another problem may occur about cutting forces. As the cutting forces are not taken into consideration, at some tool locations along the tool path, the cutting forces may exceed the feasible limit and lead to excessive tool deflection. This decreases the final part geometric accuracy, even the operation may have interrupted because of tool breakage. So, the feedrate scheduling techniques become crucial during machining operations where the cutting forces should be inspected and machining duration needs to be enhanced.

4.2.2 Case 2: 3-Axis Machining Scheduled Feedrate (Force Based)

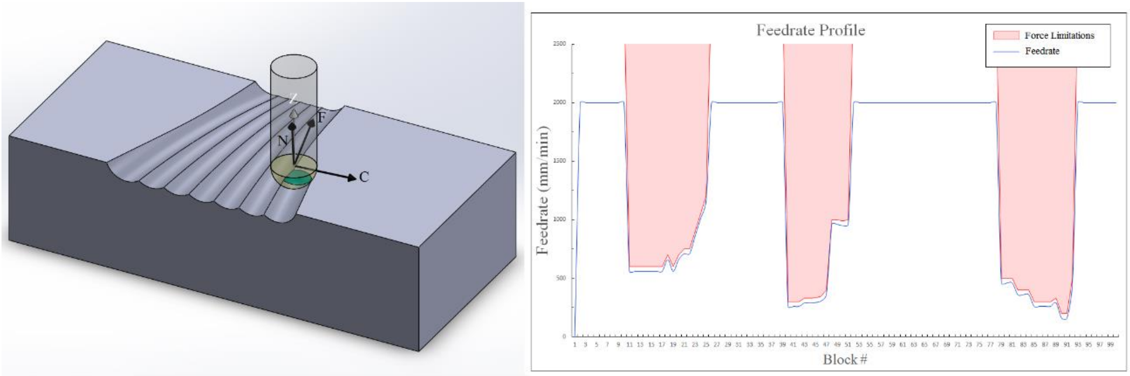

Figure 4-2: 3-Axis Machining (Force Based Feedrate Scheduling)

Case 2 is also representing a 3-axis machining operation as Case 1. However, its feedrate profile is optimized by considering the cutting forces at each CL point and readjusting the feedrate as can be seen in the graph of Figure 4-2. The feedrate is optimized for not exceeding the maximum allowed cutting force. Also a pre-defined cutting force is calculated and the feedrate value is adjusted for keeping the cutting forces constant at that value. By minimizing the maximum cutting forces, the tool deflection is decreased and the final part dimensional accuracy is ameliorated.

Cutting forces are calculated by dividing the ball end mill into differential oblique elements by the help of force model. Oblique cutting mechanics is applied on each differential element and cutting forces are predicted. Force model technique sums the differential element that are intersecting with the workpiece foe each immersion angle and calculates the resultant cutting for in both workpiece coordinate system and also tool coordinate system [29].

For cutting force calculations, normal shear angle Φ_n and normal friction angle β_n are calculated as follows where i is the oblique angle and η is the chip flow angle.

$$\tan(\phi_n) = \frac{r(\cos\eta / \cos i)\cos\alpha}{1 - r(\cos\eta / \cos i)\sin\alpha}$$

(2.3)

$$\tan(\beta_n) = \tan(\beta) * \cos\eta$$

Cutting force coefficients are found as follows:

$$K_{rc} = \frac{\tau_s}{\sin\phi_n * \cos i} * \frac{\sin(\beta_n - \alpha)}{\sqrt{\cos^2(\phi_n + \beta_n - \alpha) + \tan^2\eta * \sin^2\beta_n}}$$

$$K_{tc} = \frac{\tau_s}{\sin\phi_n} * \frac{\cos(\beta_n - \alpha) + \tan i * \tan\eta * \sin\beta_n}{\sqrt{\cos^2(\phi_n + \beta_n - \alpha_n) + \tan^2\eta * \sin^2\beta_n}} \qquad (2.4)$$

$$K_{ac} = \frac{\tau_s}{\sin\phi_n} * \frac{\cos(\beta_n - \alpha) * \tan i - \tan\eta * \sin\beta_n}{\sqrt{\cos^2(\phi_n + \beta_n - \alpha_n) + \tan^2\eta * \sin^2\beta_n}}$$

Differential cutting forces are divided into edge and shear cutting components as can be seen in Equation (2.5).

$$dF_{rj}(\phi_j, K) = K_{re} dS + K_{rc} * t(\phi_j, K) * db$$

$$dF_{tj}(\phi_j, K) = K_{te} dS + K_{tc} * t(\phi_j, K) * db \qquad (2.5)$$

$$dF_{aj}(\phi_j, K) = K_{ae} dS + K_{ac} * t(\phi_j, K) * db$$

Transformation matrix T_{xyz} is used to calculate tangential, radial and axial forces as can be seen in Equation (2.6) as follows:

$$\begin{bmatrix} dF_{xj}(\phi_j, K) \\ dF_{yj}(\phi_j, K) \\ dF_{zj}(\phi_j, K) \end{bmatrix} = \boldsymbol{T}_{xyz} \begin{bmatrix} dF_{rj}(\phi_j, z) \\ dF_{tj}(\phi_j, z) \\ dF_{aj}(\phi_j, z) \end{bmatrix} \qquad (2.6)$$

$$\boldsymbol{T}_{xyz} = \begin{bmatrix} -\sin K * \sin\phi_j & -\cos\phi_j & -\cos K * \sin\phi_j \\ -\sin K * \cos\phi_j & \sin\phi_j & -\cos K * \cos\phi_j \\ \cos K & 0 & -\sin K \end{bmatrix}$$

The cutting forces in Tool Coordinate System can be found by adding all infinitesimal forces acting on the oblique elements on the ball end milling tool for every immersion angle Φ.

$$
\begin{aligned}
F_x(\phi) &= \sum dF_{xj}(\phi_j, K) \\
F_y(\phi) &= \sum dF_{yj}(\phi_j, K) \\
F_z(\phi) &= \sum dF_{zj}(\phi_j, K)
\end{aligned}
\tag{2.7}
$$

The feedrate is adjusted to a pre-set value if the cutting force conditions are in the allowed range. However, if the cutting forces exceeds the limits, the feedrate is decreased to decrease the instantaneous cutting forces. This case can be regarded as a better approach to cutting operations however it lacks of controlling the CNC machine tools drive limitations.

4.2.3 Case 3: 3-Axis Machining Scheduled Feedrate (Feed Drive + Force Limited Model)

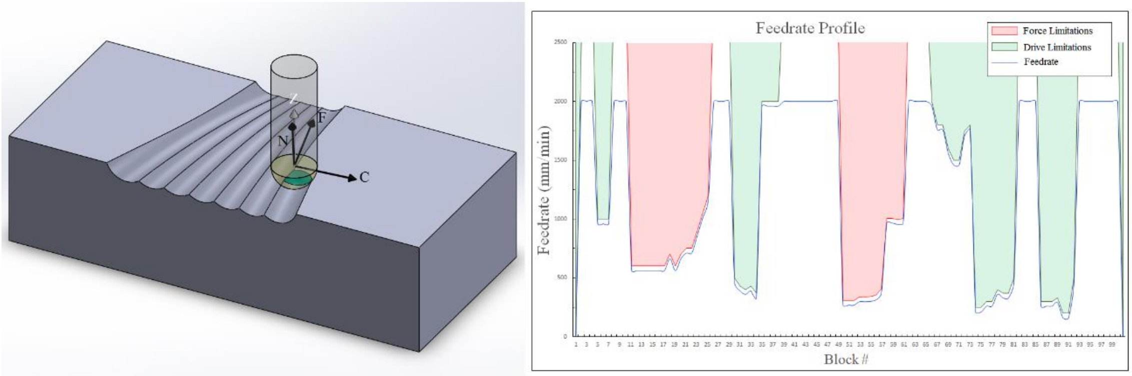

Figure 4-3: 3-Axis Machining (Limited by Feed Drive + Cutting Forces)

The approximation in Case 3 can be regarded as the best machining operation approximation. In this case all of the operation variables are inspected and controlled. At each CL point, the cutting forces are calculated with respect to CWE (Cutter Workpiece Engagement) conditions and also the requirements from each 3 axis feed drive is controlled. If the request exceeds the feed drive limitations of the CNC machine tool for the commanded motion, the feedrate is readjusted for the appropriate value for a better tracking control. As can be seen in the graph of Figure 4-3, the feedrate is adjusted at each block for remaining in the feasible region.

4.2.4 Case 4: 5-Axis Machining Constant Feedrate

Case 4 is the same as Case 1 but with addition of 2 rotary axes as seen in Figure 4-4 in the next page. The lead angle is the angle between the tool axis (Z) and the surface normal (N) in the F (Feed) direction. The tilt angle is the angle between the tool axis (Z) and the surface normal (N) in the C (Cross Feed) direction.

Both the angles can be adjusted by the help of two additional rotary axes during the operation. As this case is a more complicated one than the first three cases, cutting forces and feed drive limitations is more crucial. The cutting conditions vary dramatically in terms of tool orientation, axis velocity, cutting forces and direction, the feed drive and instantaneous cutting forces has to be considered when passed through 5-axis machining operations.

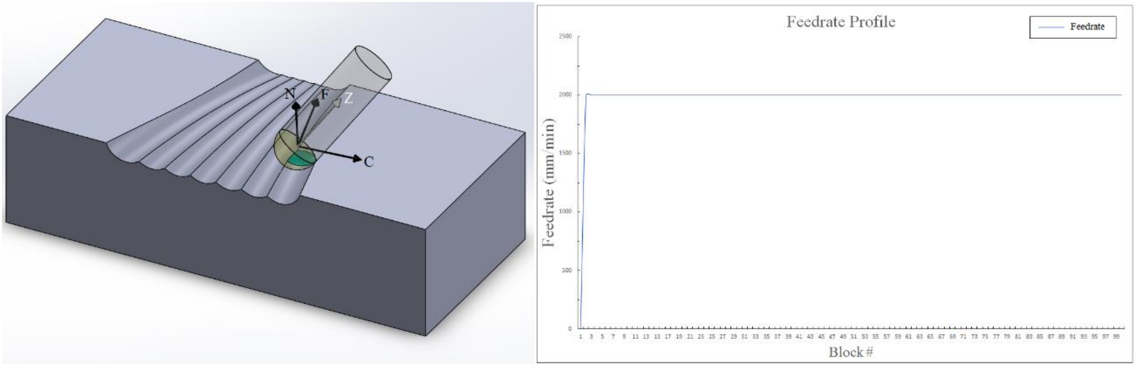

Figure 4-4: 5-Axis Machining Constant Feedrate

4.2.5 Case 5: 5-Axis Machining Scheduled Feedrate (Force Based)

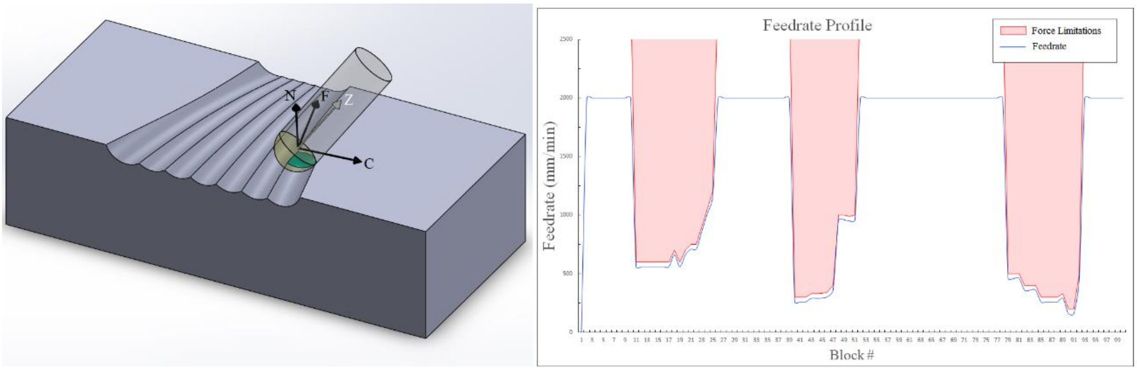

Figure 4-5:5-Axis Machining with Force Based Feedrate Scheduling

Again in this case, the feedrate value is adjusted with respect to maximum cutting forces. A predefined threshold cutting force value is calculated and the feedrate is controlled accordingly. The desired cutting force is kept constant by adjusting the feedrate. As the forces acting of the tool is kept constant, the tool deflection is stable and a part with better quality may be obtained.

4.2.6 Case 6: 5-Axis Machining (Feed Drive + Force Limited Model)

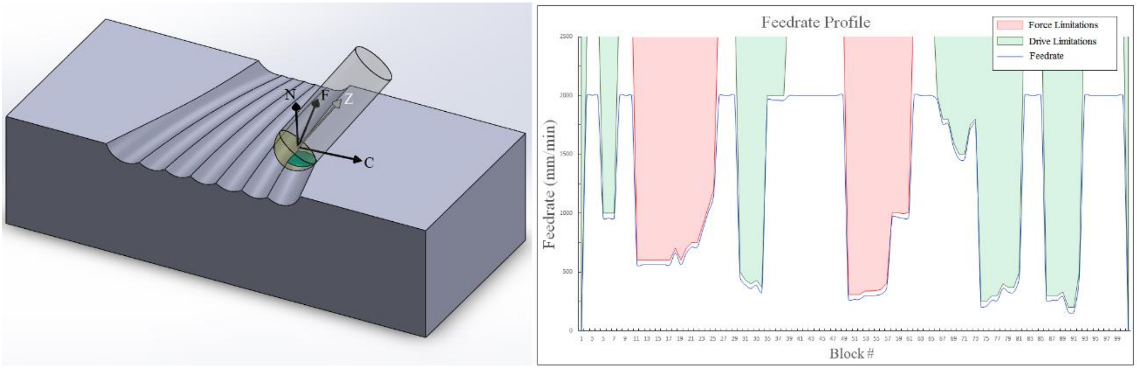

Figure 4-6: 5-Axis Machining with Lead & Tilt Angle Optimization

The Case 6 is the interested case of this study. In this case, the operation is optimized by looking at the cutting condition variables and also CNC feed drive capabilities. Optimization of lead and tilt angle variables at each CL point, lead to a better surface finish with a faster machining operation. The lead and tilt angles are kept at a certain limit which does not have an effect on the scallop heights. If the lead and tilt angles are modified without any limitations, it may affect the surface roughness value of the final product.

As the calculations gets complicated with 5-axis systems, the optimization of the operation is done in several stages. Firstly, a feasible lead and tilt angle interval is found for machining stability and optimum cutting forces. Than the feasible region is inspected for the best solution with respect to CNC drive constraints. An optimum choice is done by the algorithm in terms of lead and tilt angle combination which gives the minimum machining time. The procedure of optimization is presented in the next section.

4.3 Optimization Process Flow Chart

The study starts by choosing the workpiece that will be machined and the tool that will be used during operation as illustrated in Table 4-1. Also the stock and final geometry has to be defined but it is not shown as it is out of scope for the study of this thesis. The appropriate CAD and CAM data has to be prepared at the beginning.

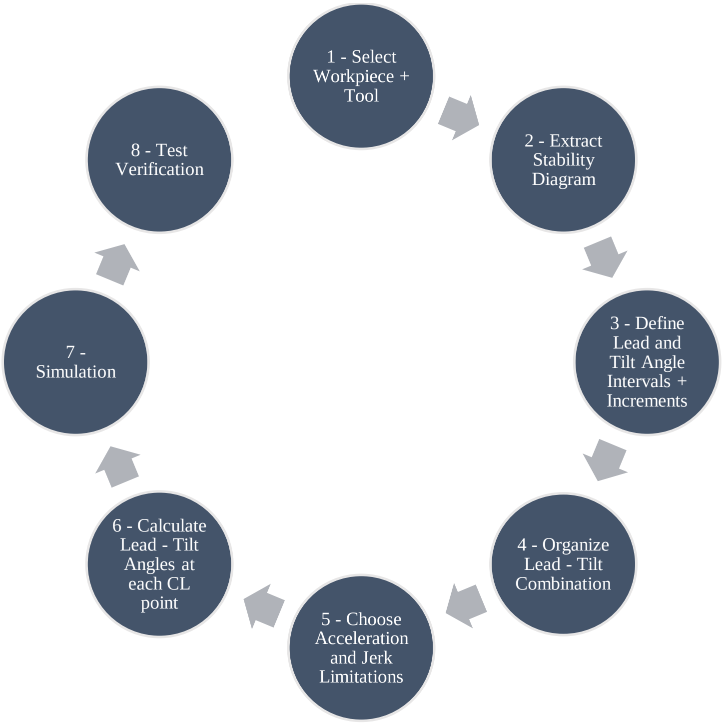

Table 4-1: Process Flow Chart for Minimization of Machining Time

By the looking at the properties of the tool and the workpiece, a stability diagram is extracted from a computer software [5] in the step 2. The feasible lead and tilt angles that can be obtained by the stability tests and an interval is defined at step 3. For instance, it can be said that the lead angle should be between 5° and 15° where the tilt angle can vary between 10° and 20°. Also the increment value should be defined, which is generally taken as 1° in this study. This increment value gives a sufficient resolution for finding the optimum answer. For each lead angle, each of the tilt angle values are tested. In other words, each combination is calculated for lead and tilt angles. The velocity, acceleration and jerk capabilities of the CNC machine tools feed drive that are measured with the tests represented in the previous chapter, are given as input to the algorithm at the step 5. In the next step, the algorithm calculates the feasibility and the amount of time that is required for each lead and tilt combination at each CL point for a given G Code. The optimum lead and tilt angles are calculated in this step with Dijkstra’s algorithm for minimizing the machining time. The algorithm chooses the shortest path from a network in which each node is feasible by the CNC machine tools drive system. The main goal is to choose the best route which will provide the shortest machining duration. A modified G Code is provided by the algorithm and it can be simulated in step 7. The same G Code is executed on a commercial CNC machine tool for verification purposes at the final step.

4.4 Solution Methodology

4.4.1 Dijkstra's Shortest Path Algorithm

The shortest path algorithm is running on a weighted graph consists of a predefined number of nodes. The main aim of the algorithm is to find the cheapest (shortest) route from initial route to the goal node. (Figure 4-7)

It assigns every node a tentative cost value which is 0 for the initial node and infinity for all other nodes. It keeps the set of visited nodes and this algorithm starts running with the initial node. When on a node, it considers all of its unvisited neighbours and calculated the distance to the current node + distance from the current node to the neighbour. If it is less than their current tentative distance, it replaces the value with the new one. When all of the neighbours are done, it marks the node as visited and gets to the new node. If the destination node is marked visited, it means that the algorithm came to the end.

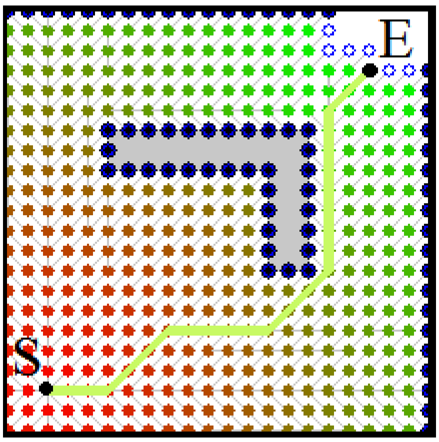

Figure 4-7: Dijkstra's Shortest Path Representation from Start Node to End Node

Dijkstra's algorithm implement in this thesis in this wise: As mentioned earlier a toolpath has various CL points which represents the tool location and orientation with respect to workpiece. At each CL location the feasible lead-tilt angle combinations are assigned. For instance, if the lead angle can vary between 6° - 10° with 1° increments and tilt angle can vary between 13° - 15° with 1° increments, the number of possible lead-tilt angle combinations would be $5\ x\ 3 = 15$. Therefore, at each CL point, 15 different lead and tilt angle combinations are assigned which can be seen as nodes in the Dijkstra's algorithm. If a toolpath has 100 CL locations on it, then there would be a 15000 x 15000 matrix in which there are all off the lead-tilt angle combinations for each CL point. The angle difference for each successive node would be the route cost. It took approximately 3 minutes to run the algorithm for a toolpath consists of 85 CL points with 121 lead-tilt (11 different lead angles & 11 different tilt angles) combinations. Dijkstra's algorithm is run on this network to minimize the tool axis rotation difference to be able to minimize the machining duration. A simple illustration of the network used in the study can be seen in Figure 4-8 below.

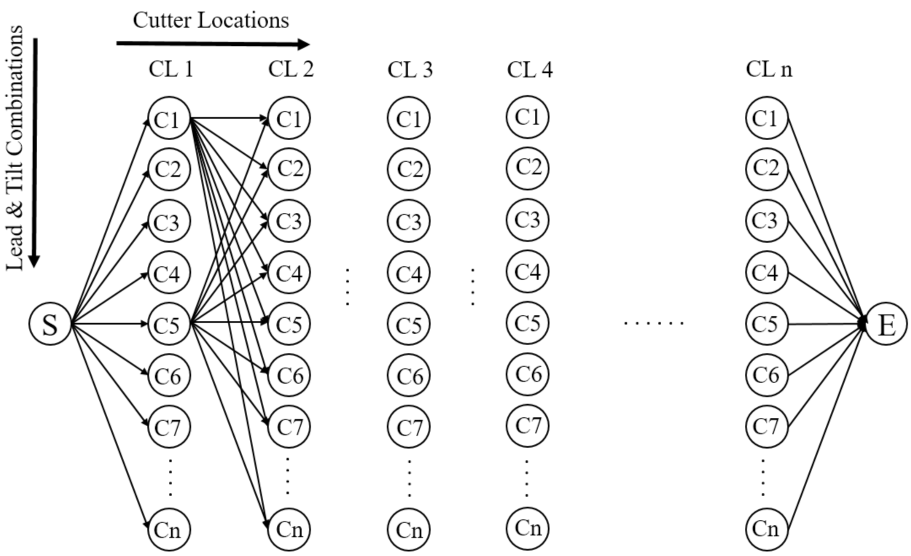

Figure 4-8: Network of Cutter Locations & Lead - Tilt Angle Combinations

The network starts with node S which is the first cutter location with predefined tool axis vectors. The columns represent CL points while rows represent the lead – tilt angle combinations for each CL point. The costs of the routes between each node is the time required to complete that displacement by the CNC machine tool axis. Required displacement for each axis is calculated in by NC commands and the highest duration of the 5 axis displacement is taken as the route cost. Algorithm tries to minimize the cumulative cost by choosing the easiest combinations to perform by the CNC machine tool.

5 CHAPTER 5 – EXPERIMENTAL RESULTS AND APPLICATIONS

5.1 Introduction

In Chapter 5, various experimental results that conducted during the study will be discussed and compared with each other. A test matrix is prepared for investigating and proving the efficiency of the proposed algorithm. The same workpiece is machined during the tests with different machining approaches that will be explained in further sections. The traditional machining results will be compared with the optimized machining approaches results. Also the proposed model simulations will be presented at the end of Chapter 5.

5.2 Experimental Results

During the study various 5-Axis machining tests are done and various parts are machined. One of the test workpieces can be seen in Figure 5-1 which is 7075 aluminum. The proposed approach is applied for tool posture optimization for cutting stability and minimum machining duration. The tool used during the tests is a 16 mm ball end mill with 4 cutting flutes and zigzag pattern applied while generating the G Code. There are 7 steps for the shown workpiece and at each step a different cutting technique is used from simplest to most complicated in order to compare.

Figure 5-1: Machined Test Workpiece

The first and second steps are machined with 3-axis machining. 3rd and 4th steps are machined with 5-axis machining and lead and tilt angles are kept constant at 0°. The steps 5 and 6 are machined with 5-axis machining whose lead and tilt angles are optimized for machining stability only. The last step which is step 7 is the result of a 5-axis machining operation which is optimized for stability and axis feed drive constraints of the CNC machine tool. All steps are compared with in other in terms of surface quality and also machining durations are recorded for each individual step.

The toolpath is generated for a zig-zag pattern machining operation as can be seen in Figure 5-2 below. Four different cutting techniques used at each step of the toolpath and steps are compared with each other which will be presented later in this section.

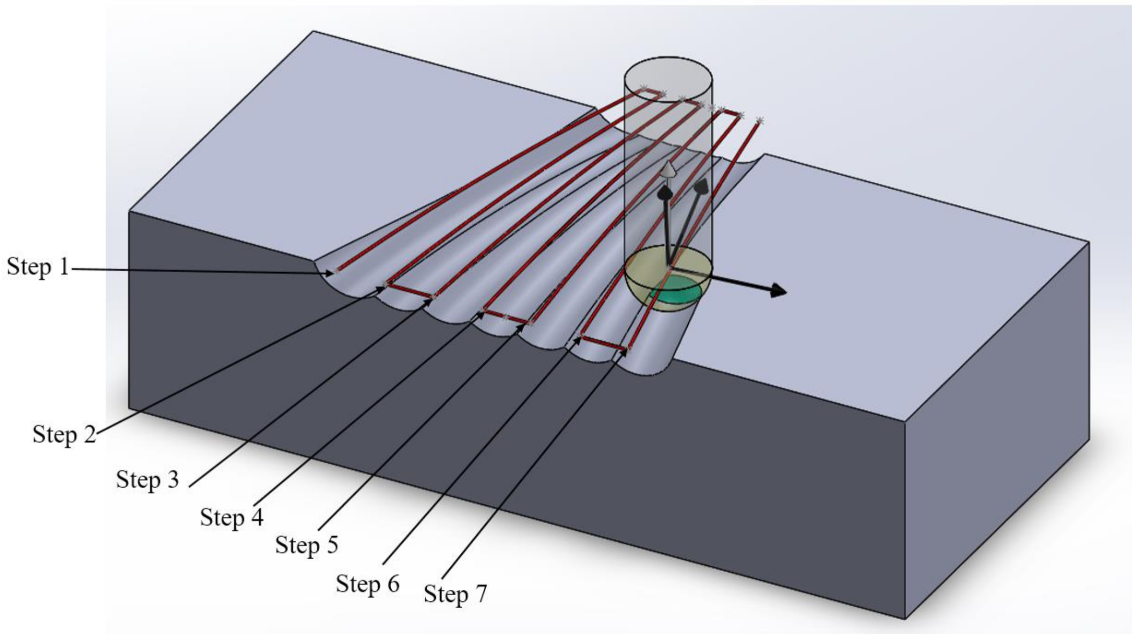

Figure 5-2: Zig-Zag Cut Pattern with 7 Steps

During the tests, cutting speed was selected as 150 m/min and the tests are conducted without coolant liquid. The spindle speed ranged between 2500 and 3000 RPM. Due to the toolpath geometry the axial depth of cut starts with 6 mm, and decreases to 2 mm at the middle of each step and it leaves the part with 4 mm axial depth of cut. Also the step over value decrease from 8 mm to 2 mm along each step. This change the stability limits along the toolpath for each step. The cutting variables are updated along each step accordingly which will be presented in this chapter in detail.

During the tests four different cutting techniques applied for comparison of the results. A general lookup table can be seen below in Table 5-1.

	Test 1	**Test 2**	**Test 3**	**Test 4**
Step #	1,2	3,4	5,6	7
Techniques Used	3 - Axis	5 - Axis	5 - Axis	5 - Axis
Lead & Tilt Angles	-	L = 0°, T = 0°	L = 10° , T = 10°	Variable
Aim	-	Stability	Stability, Min. Force	Stability, Min. Cutting Force, Min. Duration

Table 5-1: Test Layout

For the first test, Step 1 and Step 2 is machined with 3-Axis approach. The toolpath is generated with a commercial software and executed without any modifications. Due to the tool path and part geometry at the entrance to the workpiece, effective tilt angle result in chatter and the surface quality decreased significantly. The part surface can be observed in Figure 5-3. The first test is conducted for producing a surface that help to compare the efficiency of other machining approaches used in subsequent tests.

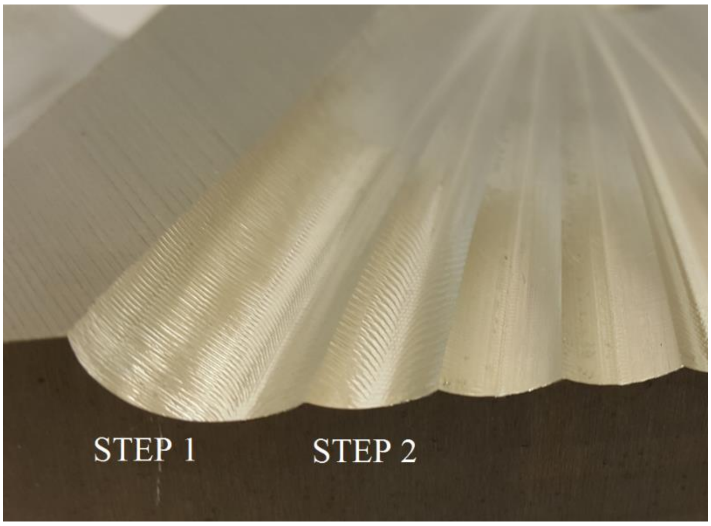

Figure 5-3: Step #1 & #2

During the second test, Step 3 and Step 4 is machined with 5-Axis machining. Lead and tilt angles kept constant at 0°. The main aim was to achieve a stable cutting operation. Although the cutting operations on Step 3 and Step 4 was stable, significant surface marks are observed which can be seen in Figure 5-4. The surface properties and comparison will be discussed later in this section. Also as the lead and tilt angles kept at 0°, the tool tip contacts left dents along the center of the toolpath which decreased the final part surface quality.

Figure 5-4: Step #3 & #4

In the third test, Step 5 and Step 6 of the toolpath are executed. The difference of this step from the other ones is that it is optimized for obtaining a stable cutting operation with stable cutting forces. The optimized cutting operation should be done while lead angle is 10° and tilt angle is 10°. The surface roughness is improved significantly in the third test as can be seen in Figure 5-6 and in the surface comparison results later in this section. However due to constant lead and tilt angles, an axis reversal from rotary axis is occurred which deteriorated the surface at the middle of the toolpath. The CNC machine tool layout cause the rotary axis to rotate 180° to keep the commanded lead and tilt angles constant. So it is concluded that this approach is not better enough too.

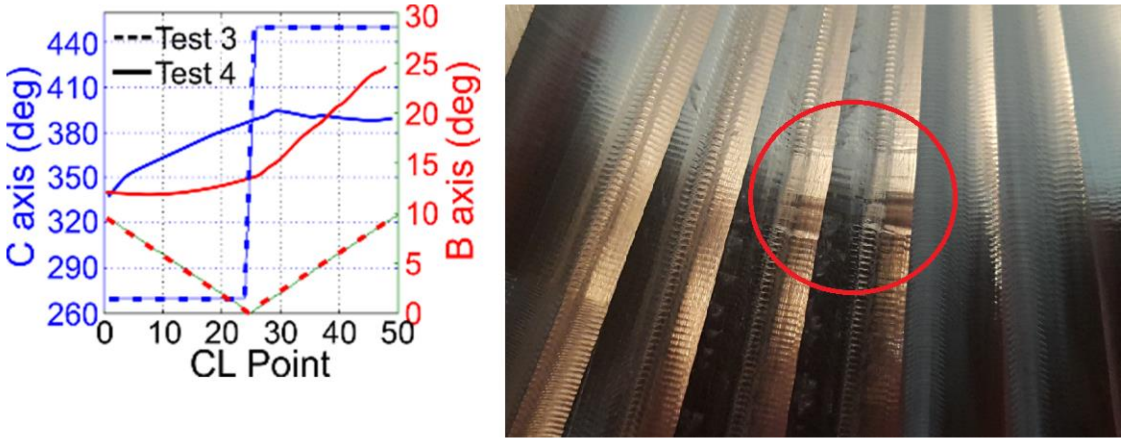

Figure 5-5: Axis Reversal occurred in Test 3 and its effects

In Figure 5-5 above, the rotary axis orientation can be observed along the toolpath. As mentioned earlier, in Test 3, the lead and tilt angle variables are kept constant at 10° which lead to axis reversal that C Axis has to rotate 180°. This phenomenon decreased the surface quality at that region Figure 5-5 and also time consuming that should be avoided.

Figure 5-6: Step #5 & #6

In the last test, Step 7 is machined with a combined approach. Instead of keeping the lead and tilt angles at a constant value, they are changed at each CL point to obtain a stable cutting + constant cutting forces and minimum rotary axis displacement which will lead the operation to a more efficient one. The surface quality increased, and machining time decreased significantly by minimizing the rotary axis movements. The Step 7 can be seen in Figure 5-7 where the dent at the beginning of the toolpath should be ignored which is formed because of misplacement of the workpiece before machining operation.

Figure 5-7: Step #7

In the last test, at each CL point, an interval of feasible lead and tilt angle combinations are assigned. Then for each combination, the required axis displacements are calculated by going from G Code to NC code. When the displacement is found, and the machine tool's axis drive limit are measured with the test presented in previous chapter, the total amount of time needed to perform that displacement can be found. The amount of time needed between each individual CL point assigned as cost between the nodes for Dijkstra's algorithm.

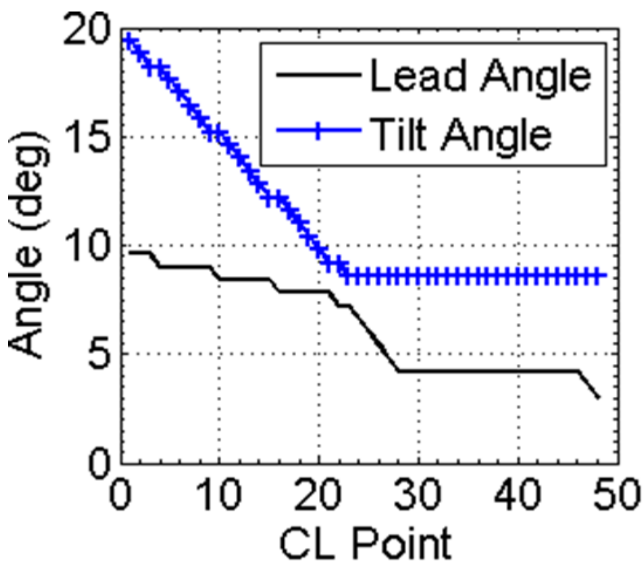

Figure 5-8: Lead & Tilt Angle Combination along Step 7

When the algorithm executed, the best lead and tilt angles combinations should be like the plot in the Figure 5-8. At the start of the toolpath, the tilt angle is selected as 20° and decreased until 10°. Whereas the lead angle is chosen as approximately 10° and decreased until approximately 3°.

Thanks to being in the stable (chatter free) region and avoiding unsmooth rotary axis displacements, the tool posture along the toolpath is optimized with the help of Dijkstra's algorithm. This lead to a smother surface finish and shorter cycle times as can be observed below successively.

5.3 Surface Investigation and Results

Surface measurements are conducted with Nanofocus μsurf explorer branded confocal microscope and Mahr MarSurf M300 C type roughness measuring instrument. A high-precision surface measurement, data and images are obtained for comparison. In this section the results from Test #2, #3 and #4 will be represented and compared with each other.

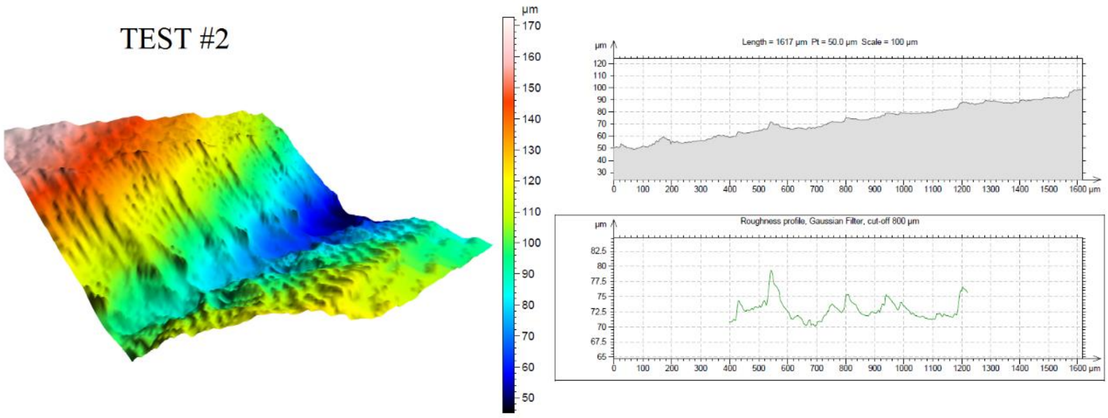

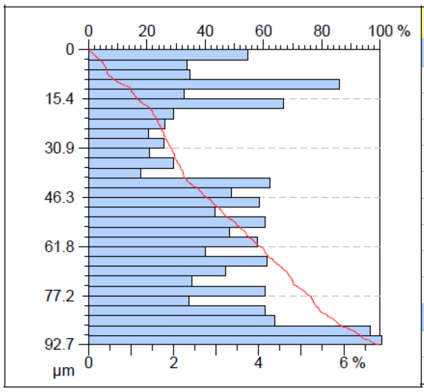

ISO 4287			
Amplitude parameters - Roughness profile			
Rp	3.76	µm	Gaussian filter, 0.8 mm
Rv	1.97	µm	Gaussian filter, 0.8 mm
Rz	5.73	µm	Gaussian filter, 0.8 mm
Rc	5.24	µm	Gaussian filter, 0.8 mm
Rt	8.80	µm	Gaussian filter, 0.8 mm
Ra	1.54	µm	Gaussian filter, 0.8 mm
Rq	1.79	µm	Gaussian filter, 0.8 mm
Rsk	1.32		Gaussian filter, 0.8 mm
Rku	2.16		Gaussian filter, 0.8 mm
Material Ratio parameters - Roughness profile			
Rmr	7.12	%	c = 1 µm under the highest peak, Gaussian filter, 0.8 mm
Rdc	3.95	µm	p = 20%, q = 80%, Gaussian filter, 0.8 mm

Figure 5-9: Surface Results from Test #2

At the left hand side of Figure 5-9 above, a 3D representation of the surface machined in Test 2 can be seen. The test is done with constant lead and tilt angles which are kept at 0°. At the bottom right of the figure above, the roughness profile can be observed. It varies between 70 μm and 80 μm, the difference is approximately 10 μm. The roughness average R_a is found as 1.54 μm with Nanofocus μsurf explorer measurement instrument.

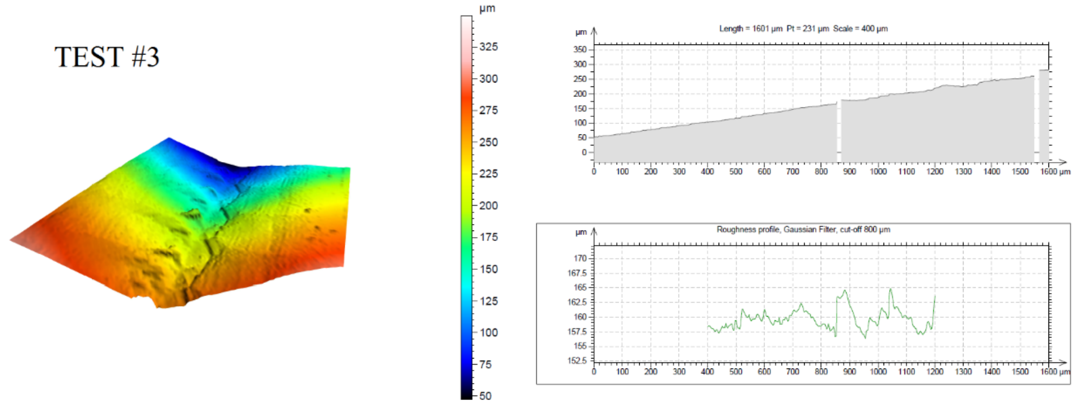

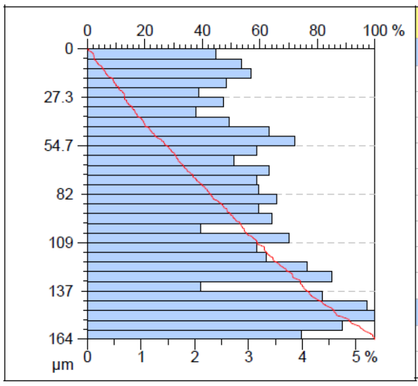

ISO 4287			
Amplitude parameters - Roughness profile			
Rp	1.53	µm	Gaussian filter, 0.8 mm
Rv	2.53	µm	Gaussian filter, 0.8 mm
Rz	4.06	µm	Gaussian filter, 0.8 mm
Rc	1.61	µm	Gaussian filter, 0.8 mm
Rt	4.06	µm	Gaussian filter, 0.8 mm
Ra	0.586	µm	Gaussian filter, 0.8 mm
Rq	0.733	µm	Gaussian filter, 0.8 mm
Rsk	-0.717		Gaussian filter, 0.8 mm
Rku	3.34		Gaussian filter, 0.8 mm
Material Ratio parameters - Roughness profile			
Rmr	29.4	%	c = 1 µm under the highest peak, Gaussian filter, 0.8 mm
Rdc	1.31	µm	p = 20%, q = 80%, Gaussian filter, 0.8 mm

Figure 5-10: Surface Results from Test #3

The Figure 5-10 above is the results from Test 3. The test 3 is conducted with constant lead and tilt angles which are kept at 10° though the toolpath step. The lead and tilt angles at this test are chosen for maximum stability. Therefore, an improvement can be seen in the roughness profile graph above. It varies between 157 µm and 164 µm and the difference is 7 µm which is 3 µm less than the previous test. Roughness average R_a is recorded as 0.586 µm for Test 3.

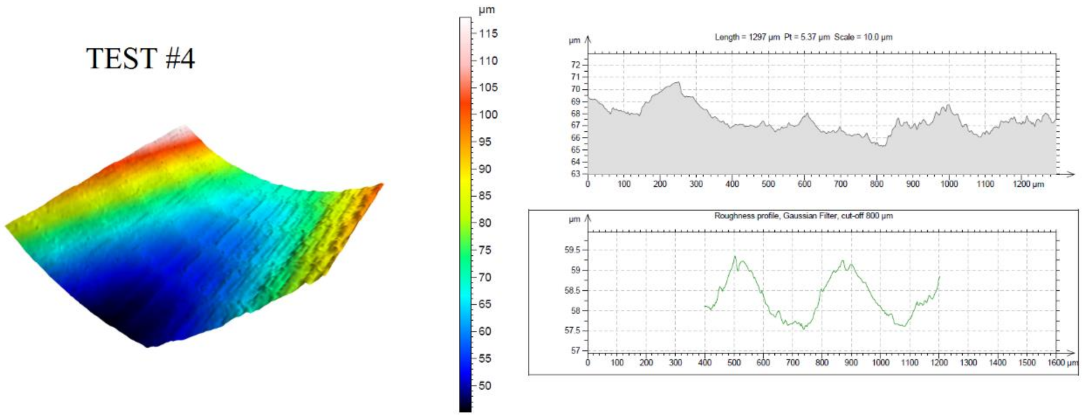

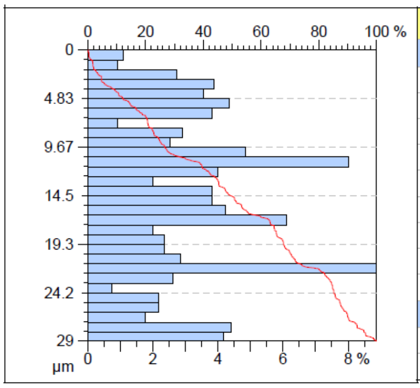

ISO 4287			
Amplitude parameters - Roughness profile			
Rp	0.937	µm	*Gaussian filter, 0.8 mm*
Rv	0.780	µm	*Gaussian filter, 0.8 mm*
Rz	1.72	µm	*Gaussian filter, 0.8 mm*
Rc	0.920	µm	*Gaussian filter, 0.8 mm*
Rt	1.72	µm	*Gaussian filter, 0.8 mm*
Ra	0.394	µm	*Gaussian filter, 0.8 mm*
Rq	0.461	µm	*Gaussian filter, 0.8 mm*
Rsk	0.242		*Gaussian filter, 0.8 mm*
Rku	2.00		*Gaussian filter, 0.8 mm*
Material Ratio parameters - Roughness profile			
Rmr	49.5	%	*c = 1 µm under the highest peak, Gaussian filter, 0.8 mm*
Rdc	0.954	µm	*p = 20%, q = 80%, Gaussian filter, 0.8 mm*

Figure 5-11: Surface Results from Test #4

In the Figure 5-11, a visible improvement on the surface can be seen in the 3D surface representation in the left hand side. Also when the surface roughness profile is observed, the graph ranges between 58 µm and 60 µm which is a significant enhancement. Thanks to the developed algorithm, surface Roughness average value R_a is 0.39 µm which is approximately 74% better than R_a value of Test 2. More detailed surface analysis reports can be found in Chapter 7.5 – Appendix E.

5.4 Proposed Model Simulations for Cycle Time Predictions

The simulations conducted with MATLAB and CUTPRO V11 simultaneously. A simple screenshot illustration can be seen below in Figure 5-12. Blue circles represent the contact locations between the tool and the workpiece while red circles represents the CL point. By calculating the vectors between the contact point and CL point, the algorithm is able to calculate tool orientation vector at each CL point.

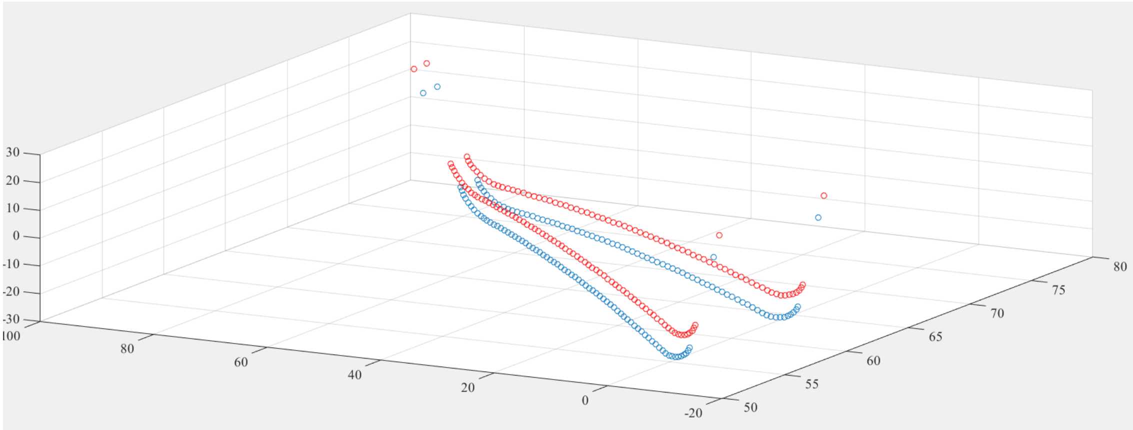

Figure 5-12: MATLAB Sample Toolpath Screenshot

For instance, the Figure 5-12 represents the toolpath for Step #5 and Step #6. The tool orientation angles are set to Lead = 10° and Tilt = 10° for maximum stability and the algorithm gave the appropriate G Code after execution.

Several test are done in the simulation and the predicted machining times are recorded for original toolpaths. After the execution of the algorithm the optimized test are simulated and the required machining time values are recorded. The predicted and real time values for original and optimized toolpaths can be seen below in Figure 5-13.

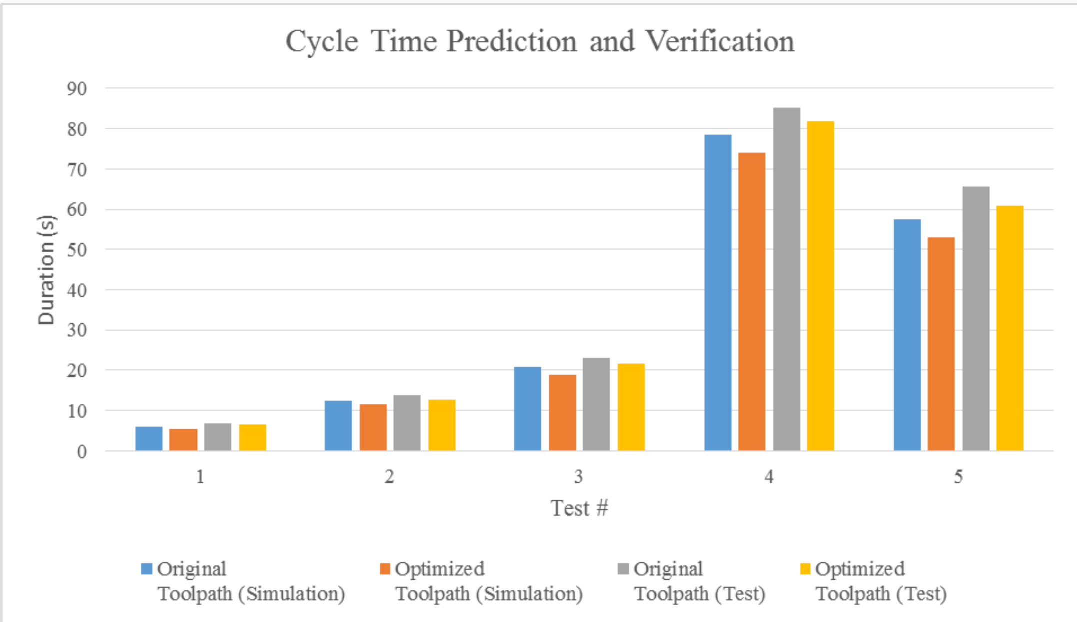

Figure 5-13: Cycle Time Prediction and Verification

The blue bars in Figure 5-13 represents the original toolpath duration prediction values by the computer simulation. Orange bars are again predicted values for optimized toolpaths. Grey bars are real machining durations that are done during the verification tests. And yellow bars are representing the optimized toolpath machining durations. It can be said that the simulation predictions are approximately 10% shorter than real time test results. This may due to unpredicted elements of the CNC machine tool that causes lags in the system. However, when the original values are compared with optimized values, there is an improvement of approximately 5% in the machining duration [28]. A more detailed table that shows cycle time values can be seen in Appendix D: Cycle times for simulation predictions and test verifications.

5.5 Summary

In Chapter 5, the approach used in this study is represented. The problem is defined and a starting point is specified. Seven different cases for feedrate optimization techniques are presented with pros and cons of each of them. Force based feedrate scheduling and feed drive limited feedrate scheduling techniques presented. At the end of the chapter, it is showed that the study in this thesis concerns with both force and drive limitations.

Optimization process flow chart is expressed with illustrations and the solution methodology is explained. Dijkstra’s shortest path algorithm help to find an optimum solution for the problem. The minimization of rotary axis movements leads to minimization of cycle time of a machining operation.

The proposed model, take a feasible lead and tilt angle interval to modify them along the toolpath to obtain a faster operation. The feasible interval is generated by looking at the stability limits of the operation and cutting force restrictions. After the feasible threshold is obtained, the algorithm selects the most efficient one to execute and generates a modified G Code. The original G Code is smoothened by smoothing rotary axis motions during G Code execution and this lead to a smoother operation by CNC machine tool. When the execution become smoother, the final part surface quality becomes smoother too as the jerky axis commands are eliminated by the algorithm.

The surface investigation results and time measurement with predictions presented. The accuracy of the model and time predictions are illustrated in the final sections of the Chapter 5.

6 CHAPTER 6 – CONCLUSIONS AND FUTURE WORK

6.1 Conclusions

Overall, this thesis has presented a novel approach for cycle time reduction in 5-Axis machining operation by optimizing the rotary axis movements according to their velocity, acceleration and jerk limitations. The proposed method results in minimum rotary axis motion that is smooth and time optimal which is optimized by looking at the CNC machine tool drive's dynamic limitations.

In 5-axis machining operations, tool axis orientation is generally selected according to workpiece geometry and most of the approaches work geometrically. However, it has many effects on the process, CNC machine tool dynamics, and final part quality and so on. Thus, the tool orientation vector has to be chosen by looking at those variables. The stability of cutting operation affects the final part surface quality and dimensional accuracy. Whereas the CNC machine tool axis drive dynamic properties affect the whole operation. When the toolpath is not generated accordingly, some unnecessary displacement commands could be executed by the CNC machine tool, which increases machining duration and also the operational costs.

The shortest path for slower rotary axis compared to linear axis is found by Dijkstra's shortest path algorithm. As the linear axis are more capable of reacting to the commanded displacements, generally the 5-axis machining operation is limited by the drive limits of the rotary axis. Thus it is crucial to improve the displacement of rotary axis during a G Code execution which will lead to an improved machining operation inherently.

To realize this improvement, the lead and tilt angle modulation over multiple toolpath intervals, at each CL point, was developed in this thesis. The lead and tilt angle modulation algorithm calculates the displacement requirements for each CL change from NC data which is generated from the G Code, and re-calculates other possible tool orientation vector requirements which may more feasible. This reduces the machining time by approximately 5% for that specific toolpath [28].

The feasibility of the algorithm is proved by machining experiments that are conducted on a commercial 5-axis CNC machine tool. The proposed method ensures that the motions of the axis are continuous and does not override acceleration and jerk limits of each axis drive system. For some toolpaths, machining duration may be reduced up to 5-6%.and surface quality is improved drastically. The enhanced motion generates approximately 30% smoother than a surface machined with regular 5-axis approach.

6.2 Suggestions for Future Work

The proposed algorithm can be implemented in production environment where the cycle times has great importance and final part quality needs to be improved or the actual quality has to be retained. The technique used in this study decreases the machining time by optimizing the G Code by looking at the axis drive characteristics. For instance, a G Code generated by a commercial software for 5-axis machining operation may command to displace a slower or lagging rotary axis more than the requirements. Thus the operation become slower which is a costly situation in production environment. The algorithm may optimize the operation to use the other faster rotary axis to compensate the lagging rotary axis to minimize the cycle time. The algorithm takes the feasible tool postures which requires to displace faster rotary axis rather than displacing slower rotary axis.

Suggestions for future work include the implementation of geometrical constraints to the algorithm. The actual technique chooses the feasible threshold by looking at the stability constraints and then the algorithm selects the most feasible one for minimum machining time. However, it would be great to implement the geometrical constraints to eliminated tool workpiece contact. The feasible interval would make more sense if it includes geometrical constraints too.

Another future suggestion may be the implementation of the algorithm into a commercial CAM software which takes the CNC machine tool axis drive limitations into consideration, thus the operation would be smoother and faster.

Also an adaptive spindle speed controller algorithm can be developed to maintain same feed per tooth value as the feedrate is adjusted instantaneously. The spindle speed may be adjusted to keep the feed per tooth value constant from the beginning of the cutting operation to make the surface quality even better.

For a better and more accurate surface finish, the scallop heights may be observed for larger lead-tilt angle intervals. The relationship between the presented algorithm and scallop height on the machined surface may be investigated in future studies.

The computational load of the algorithm may be decreased with some new constraints such as maximum allowable lead-tilt angle difference between each successive CL points for a faster solution.

7 References

[1] Altintas, Y.: Manufacturing Automation – Metal Cutting Mechanics, Machine Tool Vibrations and CNC Design, Cambridge University Press, 2000.

[2] Altintas, Y., & Erkorkmaz, K. (2003). Feedrate Optimization for Spline Interpolation In High Speed Machine Tools. CIRP Annals - Manufacturing Technology, 52(1), 297-302.

[3] Beudaert, X., Lavernhe, S., & Tournier, C. (2012). Feedrate interpolation with axis jerk constraints on 5-axis NURBS and G1 tool path. International Journal Of Machine Tools And Manufacture, 57, 73-82.

[4] Beudaert, X., Pechard, P., & Tournier, C. (2011). 5-Axis tool path smoothing based on drive constraints. International Journal Of Machine Tools And Manufacture, 51(12), 958-965.

[5] CUTPRO (Version V11). (2015). Vancouver, BC, Canada.

[6] Dong, J., Ferreira, P., & Stori, J. (2007). Feed-rate optimization with jerk constraints for generating minimum-time trajectories. International Journal Of Machine Tools And Manufacture, 47(12-13), 1941-1955.

[7] Erdim, H., Lazoglu, I., & Ozturk, B. (2006). Feedrate scheduling strategies for free-form surfaces. International Journal Of Machine Tools And Manufacture, 46(7-8), 747-757.

[8] Erkorkmaz, K., & Altintas, Y. (2001). High speed CNC system design. Part I: jerk limited trajectory generation and quintic spline interpolation. International Journal Of Machine Tools And Manufacture, 41(9), 1323-1345.

[9] Erkorkmaz, K., & Altintas, Y. (2001). High speed CNC system design. Part II: modeling and identification of feed drives. International Journal Of Machine Tools And Manufacture, 41(10), 1487-1509.

[10] Erkorkmaz, K., Layegh, S., Lazoglu, I., & Erdim, H. (2013). Feedrate optimization for freeform milling considering constraints from the feed drive system and process mechanics. CIRP Annals - Manufacturing Technology, 62(1), 395-398.

[11] Ernesto, C., & Farouki, R. (2011). High-speed cornering by CNC machines under prescribed bounds on axis accelerations and toolpath contour error. The International Journal Of Advanced Manufacturing Technology, 58(1-4), 327-338.

[12] Fussell, B., & Srinivasan, K. (1989). An Investigation of the End Milling Process Under Varying Machining Conditions. Journal Of Engineering For Industry, 111(1), 27.

[13] Fussell, B.K., C. Ersoy, R.B. Jerard, "Computer Generated CNC Machining Feedrates,", USA/Japan Symposium on Flexible Manufacturing, San Francisco, July 13-15, 1992.

[14] Fussell, B.K., R.B. Jerard and O.K. Durdag, "Geometric and Mechanistic Model Integration for 3-Axis CNC Feedrate Generation," ASME Winter Annual Meeting, San Francisco, Dec. 1995.

[15] Fussell, B.K. R.B. Jerard and J.G. Hemmett, "CNC Feed Velocity Selection for Sculptured Surface Machining," Proceedings of the 2000 NSF Design and Manufacturing System Conference," Vancouver, B.C., Canada, Jan. 3-6.

[16] Heng, M., & Erkorkmaz, K. (2010). Design of a NURBS interpolator with minimal feed fluctuation and continuous feed modulation capability. International Journal Of Machine Tools And Manufacture, 50(3), 281-293.

[17] Jerard, R., Fussell, B., Hemmet, J., & Ercan, M. (2000). Toolpath Feedrate Optimization: A Case Study. Proceedings of The 2000 NSF Design & Manufacturing Research Conference, Jan 3-6, 2000.

[18] Lee, A., Lin, M., Pan, Y., & Lin, W. (2011). The feedrate scheduling of NURBS interpolator for CNC machine tools. Computer-Aided Design, 43(6), 612-628.

[19] Nam, S., & Yang, M. (2004). A study on a generalized parametric interpolator with real-time jerk-limited acceleration. Computer-Aided Design, 36(1), 27-36.

[20] Ozturk, E., Tunc, L., & Budak, E. (2009). Investigation of lead and tilt angle effects in 5-axis ball-end milling processes. International Journal Of Machine Tools And Manufacture, 49(14), 1053-1062.

[21] Ozturk,E., Budak,E., Modeling of 5-axis milling processes, Machining Science and Technology 11(3)(2007)287–311.

[22] Sencer, B., Altintas, Y., & Croft, E. (2008). Feed optimization for five-axis CNC machine tools with drive constraints. International Journal Of Machine Tools And Manufacture, 48(7-8), 733-745.

[23] Takata, S., Tsai, M., Inui, M., & Sata, T. (1989). A Cutting Simulation System for Machinability Evaluation Using a Workpiece Model. *CIRP Annals - Manufacturing Technology*, *38*(1), 417-420.

[24] Timar, S., & Farouki, R. (2007). Time-optimal traversal of curved paths by Cartesian CNC machines under both constant and speed-dependent axis acceleration bounds. Robotics And Computer-Integrated Manufacturing, 23(5), 563-579.

[25] Tounsi, N., Bailey, T., & Elbestawi, M. (2003). Identification of acceleration deceleration profile of feed drive systems in CNC machines. International Journal Of Machine Tools And Manufacture, 43(5), 441-451.

[26] Zhou, J., Sun, Y., & Guo, D. (2014). Adaptive feedrate interpolation with multiconstraints for five-axis parametric toolpath. The International Journal Of Advanced Manufacturing Technology, 71(9-12), 1873-1882.

[27] Volume Based Feed Rate Optimization: Can We Rely On It?. (2011). [Blog] Available at: http://www.terranicsystems.com [Accessed 10 Feb. 2016].

[28] Bilgen, S., Ozlu, E., Erberdi. M.S., & Budak, E. (2015). An Experimental Study of CNC Machine Tool Feed Drive Limits and Cycle Time Prediction for 3-Axis Milling Operation. *8th International Conference and Exhibition on Design and Production of MACHINES and DIES/MOLDS*

[29] Öztürk, Erdem and Erhan Budak. Modeling Of 5-Axis Milling Forces And Form Errors, 2005. Print.

7.1 Appendix A: Linear Axis (X – Y – Z) Measurement Data (Velocity – Acceleration – Jerk – Duration)

X-Axis 5mm

Calculated	Given	Measured					
Est. Velocity	Feed	X-Velocity	X-Acceleration		X-Jerk		Duration (X)
m/s	mm/min	m/s	m/s2	G	m/s3	G/s	s
0.0017	100	0.0017	0.0334	0.0034	1.3578	0.1384	3.0236
0.0083	500	0.0084	0.1419	0.0145	5.2051	0.5306	0.6669
0.0167	1000	0.0167	0.2875	0.0293	6.5012	0.6627	0.3704
0.0250	1500	0.0251	0.4485	0.0457	12.3029	1.2541	0.2691
0.0333	2000	0.0334	0.5483	0.0559	14.4221	1.4701	0.2432
0.0417	2500	0.0413	0.6568	0.0671	16.7057	1.7029	0.2216
0.0500	3000	0.0488	0.7587	0.0773	19.6888	2.0070	0.1976
0.0583	3500	0.0547	0.9073	0.0925	21.5611	2.1978	0.1856
0.0667	4000	0.0550	0.9515	0.0970	22.5486	2.2985	0.1843
0.0750	4500	0.0557	0.8981	0.0915	21.0685	2.1477	0.1881
0.0833	5000	0.0570	0.9942	0.1013	21.7265	2.2147	0.1857
0.0917	5500	0.0551	0.9541	0.0973	21.2741	2.1686	0.1864
0.1000	6000	0.0572	0.9865	0.1006	21.9932	2.2419	0.1856
0.1083	6500	0.0553	0.9551	0.0974	20.9644	2.1370	0.1866
0.1167	7000	0.0561	0.9747	0.0994	22.1988	2.2628	0.1874

Table 7-1: X - Axis Linear Measurement Data

Y-Axis 5mm

Calculated	Given	Measured					
Est. Velocity	Feed	Y-Velocity	Y-Acceleration		Y-Jerk		Duration (Y)
m/s	mm/min	m/s	m/s2	G	m/s3	G/s	s
0.0017	100	0.0019	0.0283	0.0029	0.9863	0.1005	3.0101
0.0083	500	0.0084	0.1605	0.0164	3.8678	0.3943	0.6521
0.0167	1000	0.0168	0.2777	0.0283	8.7437	0.8913	0.4011
0.0250	1500	0.0252	0.4356	0.0444	12.2412	1.2478	0.2817
0.0333	2000	0.0334	0.5637	0.0575	14.4865	1.4767	0.2207
0.0417	2500	0.0414	0.7036	0.0717	16.5402	1.6861	0.2120
0.0500	3000	0.0487	0.7803	0.0795	19.0722	1.9442	0.1902
0.0583	3500	0.0533	0.8656	0.0882	20.4090	2.0804	0.1901
0.0667	4000	0.0565	0.9305	0.0948	22.1988	2.2629	0.1742
0.0750	4500	0.0568	0.9983	0.1018	21.4785	2.1895	0.1715
0.0833	5000	0.0570	0.9958	0.1015	20.9850	2.1391	0.1886
0.0917	5500	0.0549	0.9032	0.0921	22.3635	2.2797	0.1862
0.1000	6000	0.0565	0.9346	0.0953	22.4251	2.2860	0.1802
0.1083	6500	0.0565	0.9361	0.0954	22.6514	2.3090	0.1751
0.1167	7000	0.0567	0.9865	0.1006	22.4041	2.2838	0.1713

Table 7-2: Y - Axis Linear Measurement Data

Z-Axis		Calculated	Given	Measured					
5mm		Est. Velocity	Feed	Z-Velocity	Z-Acceleration		Z-Jerk		Duration (Z)
		m/s	mm/min	m/s	m/s2	G	m/s3	G/s	s
		0.0017	100	0.0018	0.0298	0.0030	0.6986	0.0712	3.0634
		0.0083	500	0.0085	0.1605	0.0164	0.0164	0.3439	0.6514
		0.0167	1000	0.0168	0.2999	0.0306	7.4501	0.7594	0.3667
		0.0250	1500	0.0251	0.4171	0.0425	11.1302	1.1346	0.2686
		0.0333	2000	0.0332	0.5899	0.0601	12.3852	1.2625	0.2290
		0.0417	2500	0.0414	0.7026	0.0716	15.6782	1.5982	0.2111
		0.0500	3000	0.0481	0.8065	0.0822	17.6520	1.7994	0.1978
		0.0583	3500	0.0540	0.9294	0.0947	20.3483	2.0742	0.1901
		0.0667	4000	0.0561	0.9047	0.0922	22.1166	2.2545	0.1899
		0.0750	4500	0.0558	0.9639	0.0964	21.6433	2.2063	0.1843
		0.0833	5000	0.0546	0.9016	0.0919	21.2731	2.1685	0.1833
		0.0917	5500	0.0566	0.9356	0.0954	21.5611	2.1979	0.1730
		0.1000	6000	0.0562	0.9181	0.0936	21.7051	2.2126	0.1742
		0.1083	6500	0.0549	0.8965	0.0914	21.5211	2.1937	0.1790
		0.1167	7000	0.0543	0.9068	0.0924	21.1703	2.1580	0.1725

Table 7-3: Z - Axis Linear Measurement Data

7.2 Appendix B: Rotary Axis (B – C) Measurement Data (Velocity – Acceleration – Jerk – Duration)

B-Axis	Calculated	Given	Measured				
1 deg	Est. Velocity	Feed	B-Velocity	B-Acceleration		B-Jerk	
	°/s	sec	°/s	°/s2	G	°/s3	G/s
	0.0250	1/40	0.0224	0.7816	0.0797	38.8778	3.9631
	0.1250	1/8	0.1118	3.9580	0.4035	185.2689	18.8857
	0.2000	1/5	0.2031	6.9676	0.7103	256.7844	26.1758
	0.2500	1/4	0.2269	6.7133	0.6843	464.9978	47.4004
	0.3333	1/3	0.2253	6.7251	0.6855	459.1889	46.8082
	0.5000	1/2	0.2176	7.0848	0.7222	440.8511	44.9390
	1.0000	1/1	0.2256	7.1838	0.7323	418.5356	42.6642

Table 7-4: B - Axis Rotary Measurement Data

C-Axis	Calculated	Given	Measured				
1 deg	Est. Velocity	Feed	C-Velocity	C-Acceleration		C-Jerk	
	°/s	sec	°/s	°/s2	G	°/s3	G/s
	0.0250	1/40	0.0315	0.9447	0.0963	66.1459	6.7427
	0.1250	1/8	0.1425	3.7575	0.3830	290.2325	29.5854
	0.2000	1/5	0.2750	6.9297	0.7064	385.4031	39.2868
	0.2500	1/4	0.2617	6.9735	0.7109	485.8322	49.5242
	0.3333	1/3	0.2700	7.3253	0.7467	474.9000	48.4098
	0.5000	1/2	0.2649	6.9498	0.7084	489.8819	49.9370
	1.0000	1/1	0.2711	7.0244	0.7160	491.3938	50.0911

Table 7-5: C - Axis Rotary Measurement Data

7.3 Appendix C: Laser Interferometer Test Results

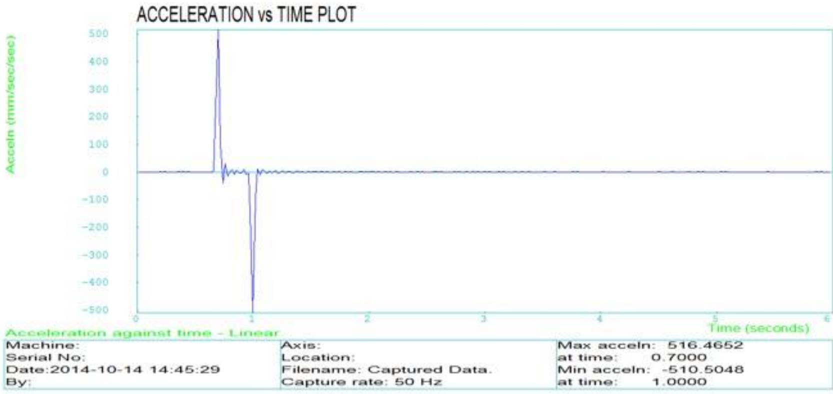

Figure 7-1: Acceleration Profile for 1000 mm/min feedrate

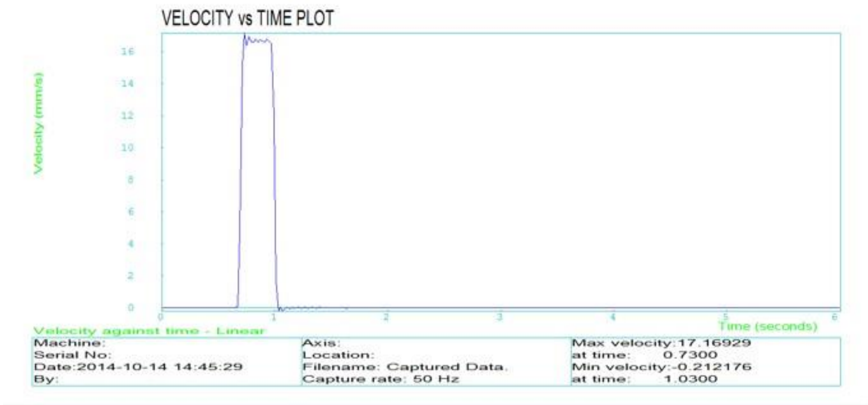

Figure 7-2: Velocity Profile for 1000 mm/min feedrate

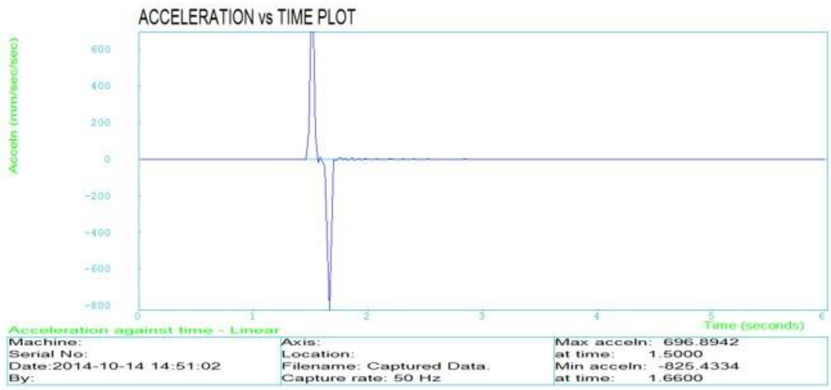

Figure 7-3: Acceleration Profile for 2000 mm/min feedrate

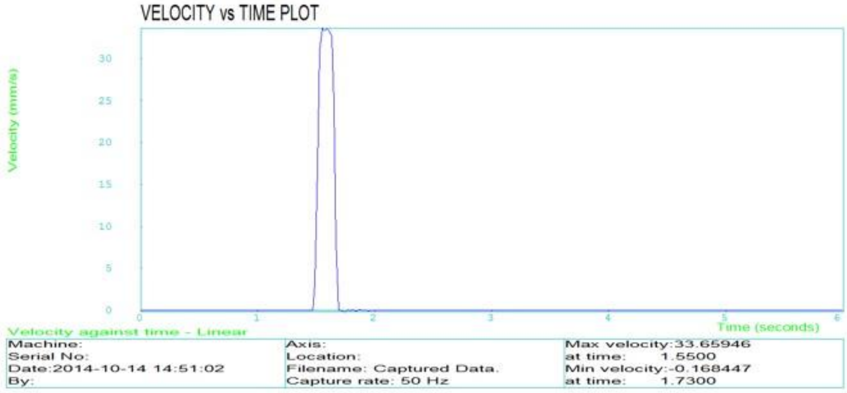

Figure 7-4: Velocity Profile for 2000 mm/min feedrate

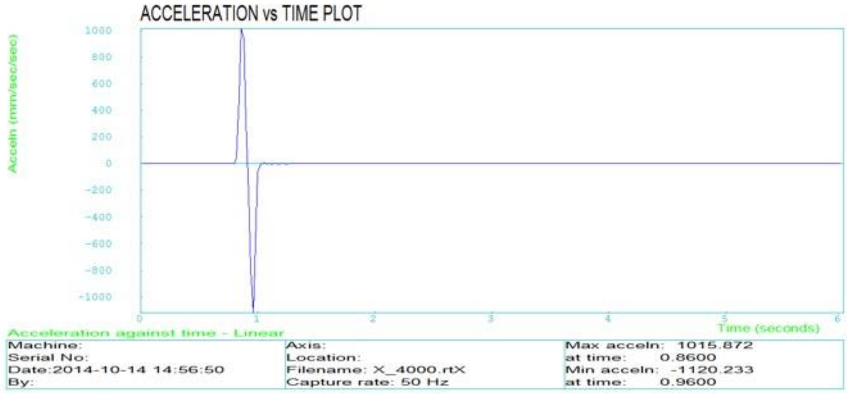

Figure 7-5: Acceleration Profile for 4000 mm/min feedrate

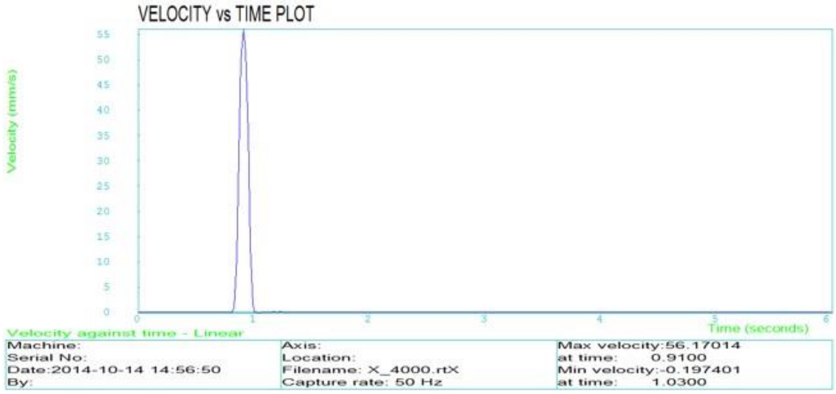

Figure 7-6: Velocity Profile for 4000 mm/min feedrate

7.4 Appendix D: Cycle times for simulation predictions and test verifications

	Predicted with Simulation		Verified with Tests	
Test #	Original Toolpath	Optimized Toolpath	Original Toolpath (Test)	Optimized Toolpath (Test)
1	6.01	5.56	6.84	6.48
2	12.35	11.67	13.97	12.82
3	20.71	18.92	23.14	21.74
4	78.57	73.98	85.31	81.908
5	57.62	53.08	65.61	60.91
			* all data is in seconds.	

7.5 Appendix E: Detailed Reports for Machined Surfaces

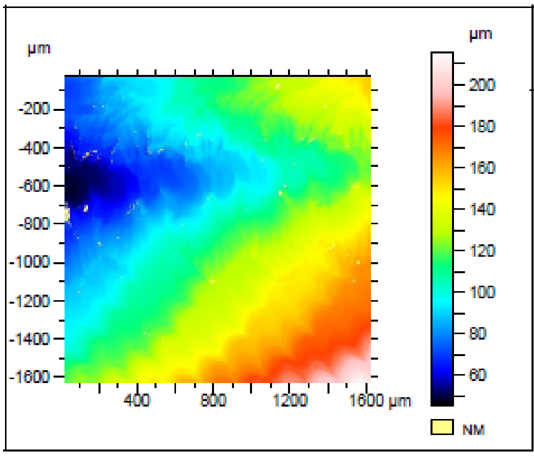

STEP 1

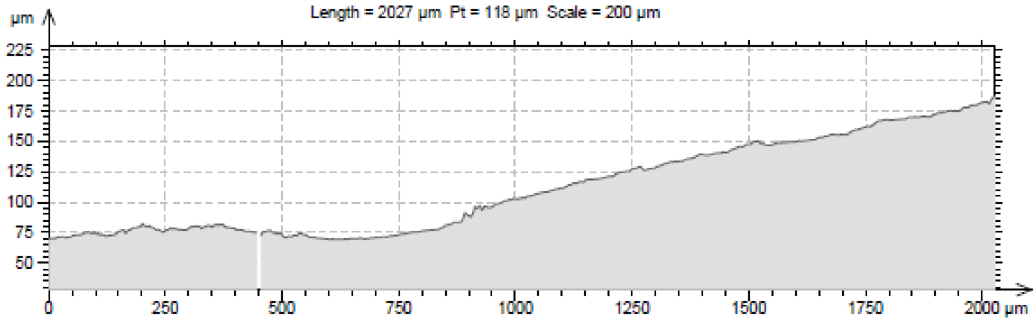

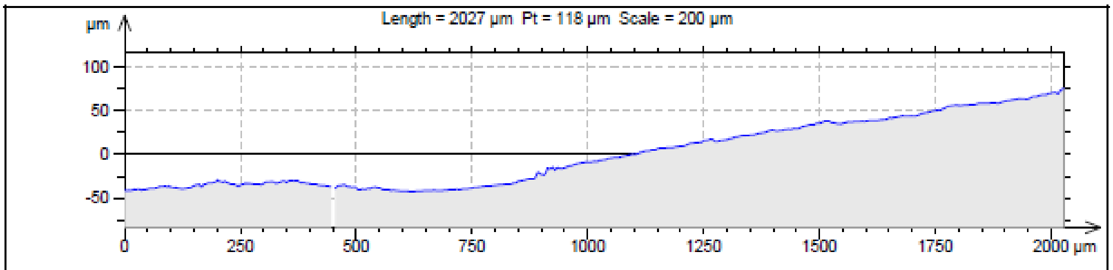

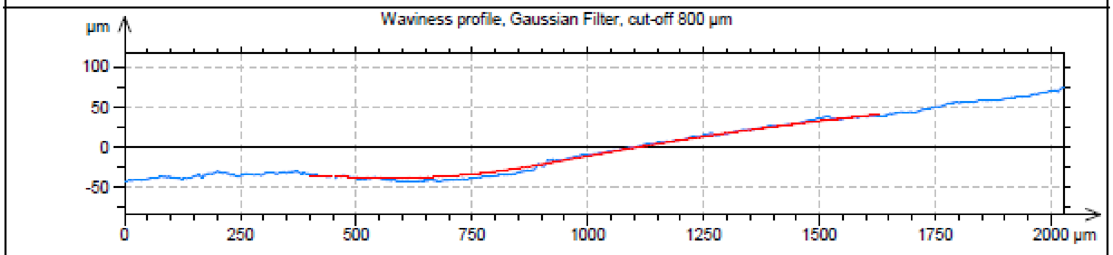

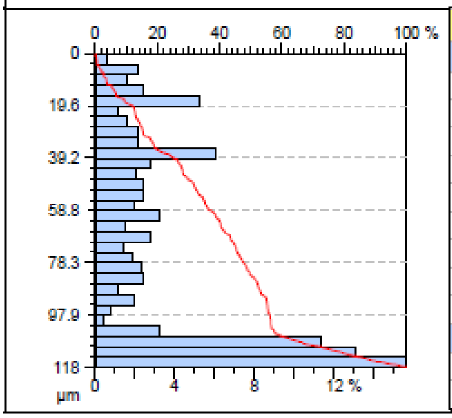

ISO 4287			
Amplitude parameters - Roughness profile			
Rp	4.70	µm	Gaussian filter, 0.8 mm
Rv	5.74	µm	Gaussian filter, 0.8 mm
Rz	10.4	µm	Gaussian filter, 0.8 mm
Rc	5.29	µm	Gaussian filter, 0.8 mm
Rt	11.0	µm	Gaussian filter, 0.8 mm
Ra	2.71	µm	Gaussian filter, 0.8 mm
Rq	3.04	µm	Gaussian filter, 0.8 mm
Rsk	-0.843		Gaussian filter, 0.8 mm
Rku	1.71		Gaussian filter, 0.8 mm
Material Ratio parameters - Roughness profile			
Rmr	2.18	%	c = 1 µm under the highest peak, Gaussian filter, 0.8 mm
Rdc	5.83	µm	p = 20%, q = 80%, Gaussian filter, 0.8 mm

STEP 4 - AXIS REVERSAL START

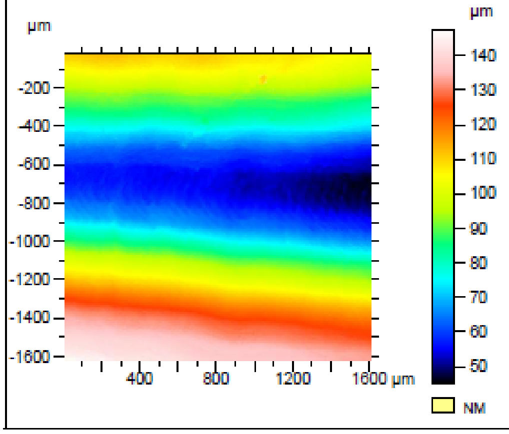

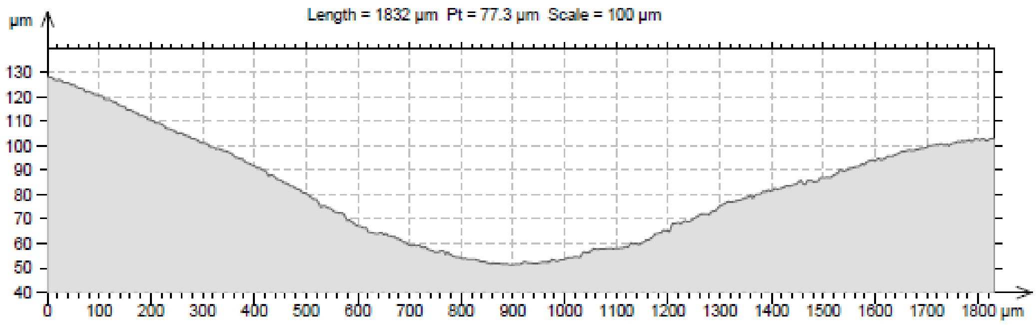

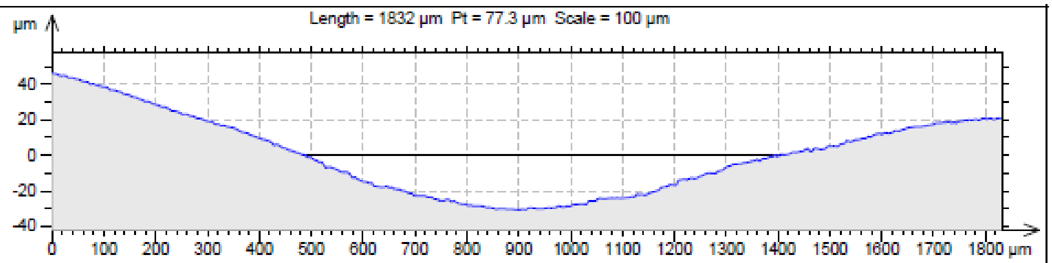

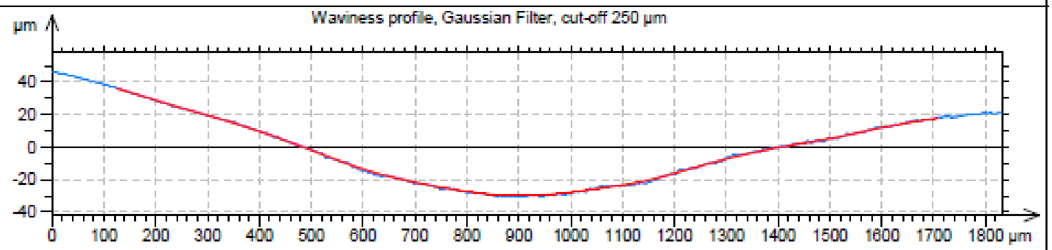

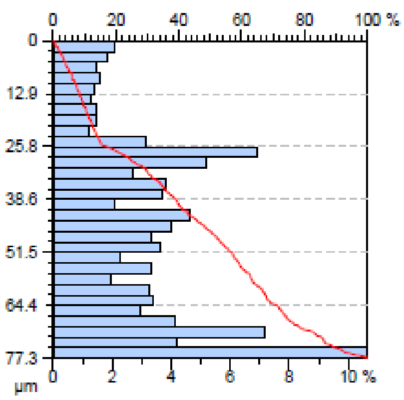

ISO 4287			
Amplitude parameters - Roughness profile			
Rp	3.27	µm	*Gaussian filter, 0.8 mm*
Rv	2.79	µm	*Gaussian filter, 0.8 mm*
Rz	6.07	µm	*Gaussian filter, 0.8 mm*
Rc	2.83	µm	*Gaussian filter, 0.8 mm*
Rt	6.73	µm	*Gaussian filter, 0.8 mm*
Ra	1.50	µm	*Gaussian filter, 0.8 mm*
Rq	1.69	µm	*Gaussian filter, 0.8 mm*
Rsk	-0.417		*Gaussian filter, 0.8 mm*
Rku	1.68		*Gaussian filter, 0.8 mm*
Material Ratio parameters - Roughness profile			
Rmr	10.5	%	*c = 1 µm under the highest peak, Gaussian filter, 0.8 mm*
Rdc	4.03	µm	*p = 20%, q = 80%, Gaussian filter, 0.8 mm*

STEP 4 - AXIS REVERSAL EXIT

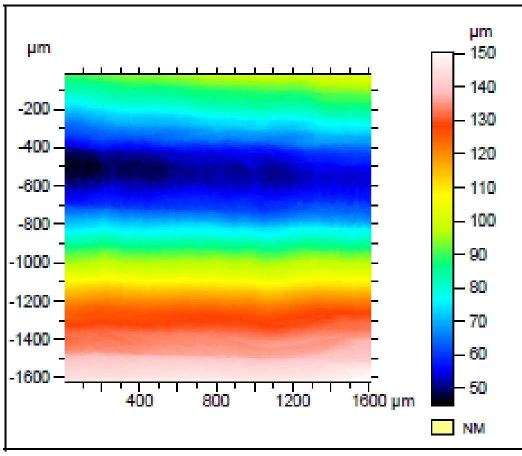

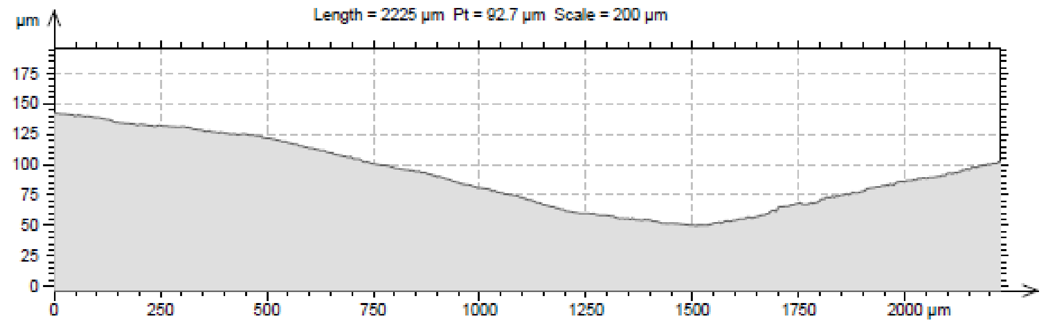

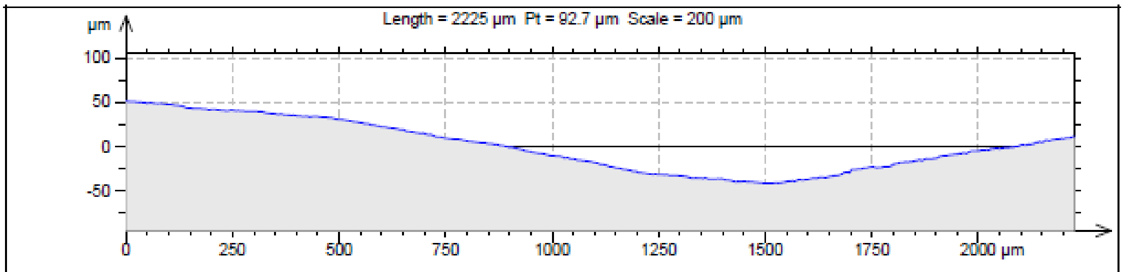

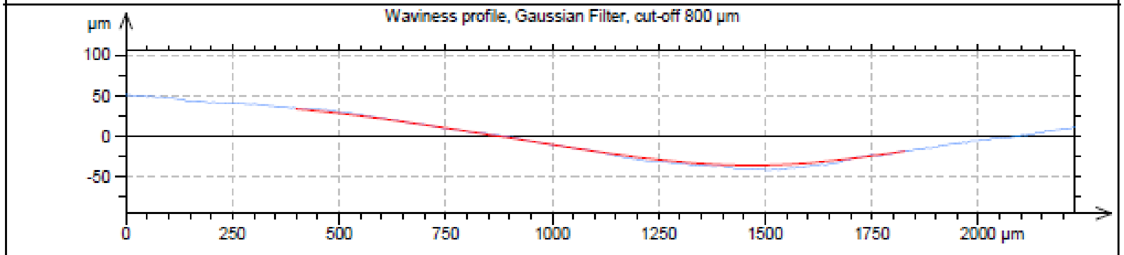

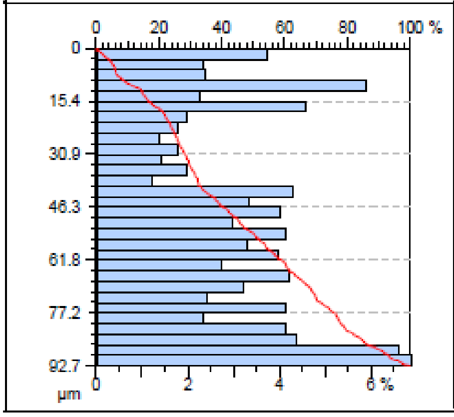

ISO 4287			
Amplitude parameters - Roughness profile			
Rp	3.76	µm	*Gaussian filter, 0.8 mm*
Rv	1.97	µm	*Gaussian filter, 0.8 mm*
Rz	5.73	µm	*Gaussian filter, 0.8 mm*
Rc	5.24	µm	*Gaussian filter, 0.8 mm*
Rt	8.80	µm	*Gaussian filter, 0.8 mm*
Ra	1.54	µm	*Gaussian filter, 0.8 mm*
Rq	1.79	µm	*Gaussian filter, 0.8 mm*
Rsk	1.32		*Gaussian filter, 0.8 mm*
Rku	2.16		*Gaussian filter, 0.8 mm*
Material Ratio parameters - Roughness profile			
Rmr	7.12	%	*c = 1 µm under the highest peak, Gaussian filter, 0.8 mm*
Rdc	3.95	µm	*p = 20%, q = 80%, Gaussian filter, 0.8 mm*

STEP 5

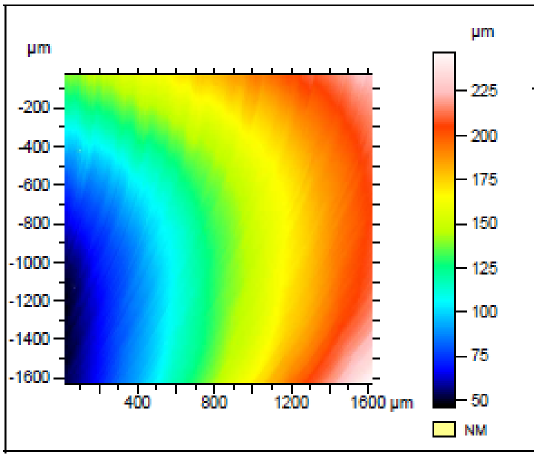

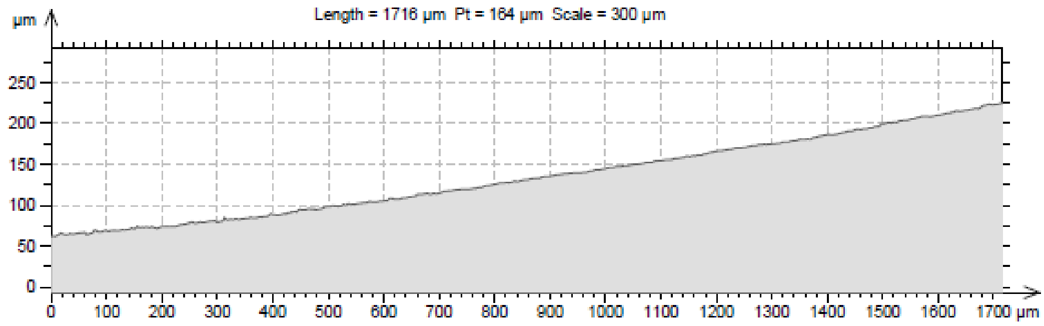

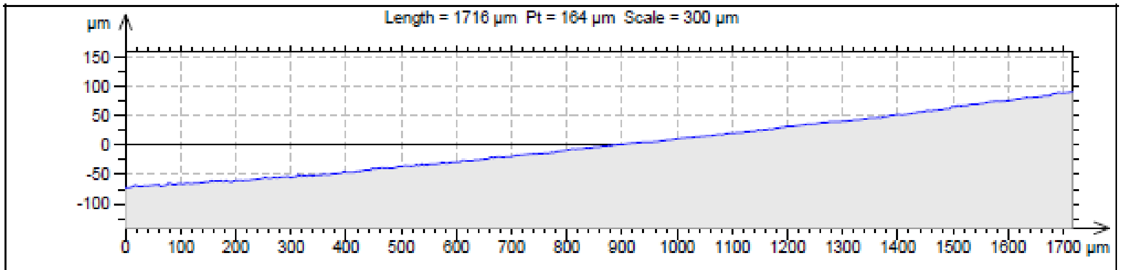

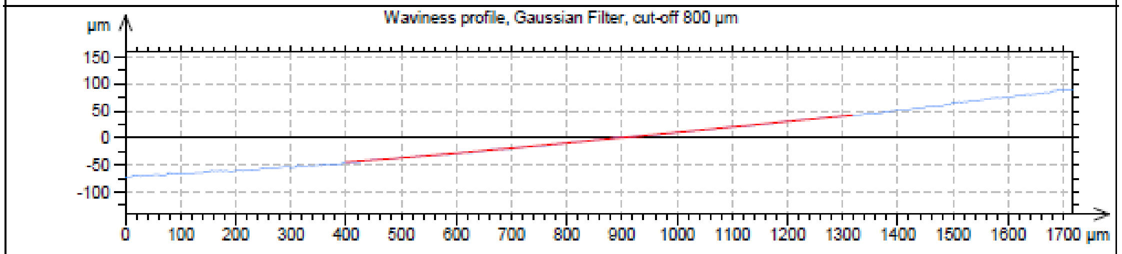

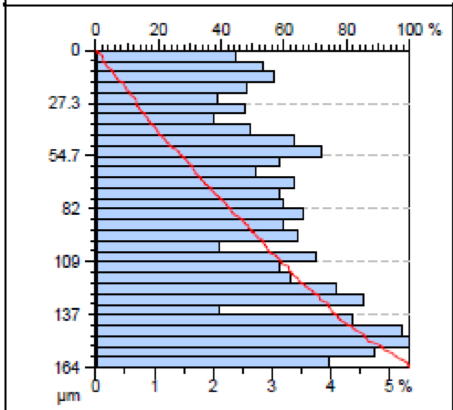

ISO 4287			
Amplitude parameters - Roughness profile			
Rp	1.53	µm	*Gaussian filter, 0.8 mm*
Rv	2.53	µm	*Gaussian filter, 0.8 mm*
Rz	4.06	µm	*Gaussian filter, 0.8 mm*
Rc	1.61	µm	*Gaussian filter, 0.8 mm*
Rt	4.06	µm	*Gaussian filter, 0.8 mm*
Ra	0.586	µm	*Gaussian filter, 0.8 mm*
Rq	0.733	µm	*Gaussian filter, 0.8 mm*
Rsk	-0.717		*Gaussian filter, 0.8 mm*
Rku	3.34		*Gaussian filter, 0.8 mm*
Material Ratio parameters - Roughness profile			
Rmr	29.4	%	*c = 1 µm under the highest peak, Gaussian filter, 0.8 mm*
Rdc	1.31	µm	*p = 20%, q = 80%, Gaussian filter, 0.8 mm*

STEP 7

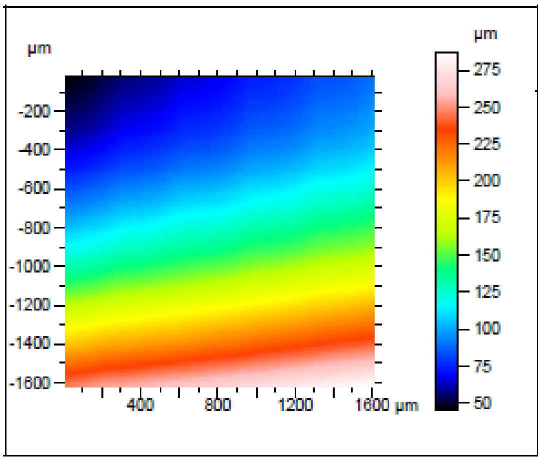

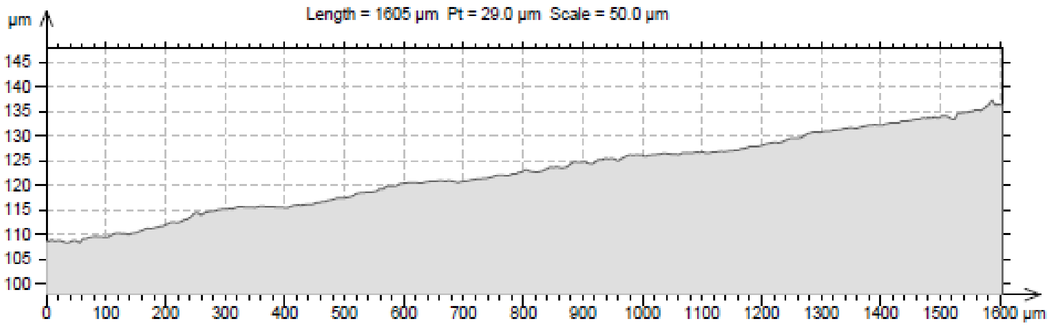

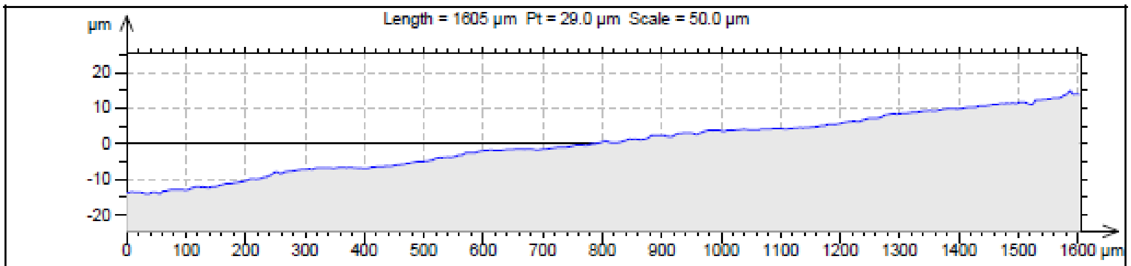

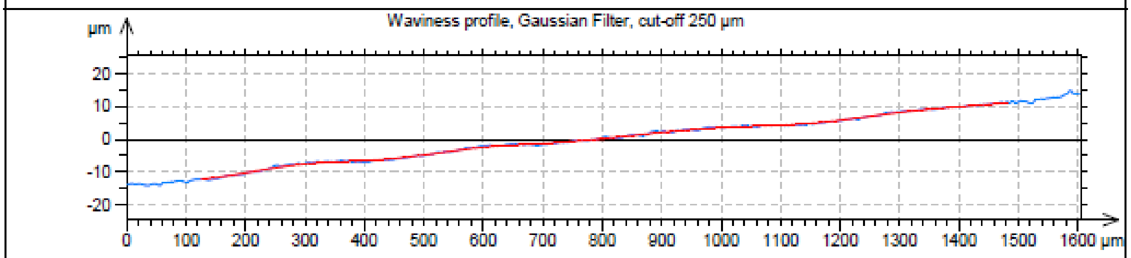

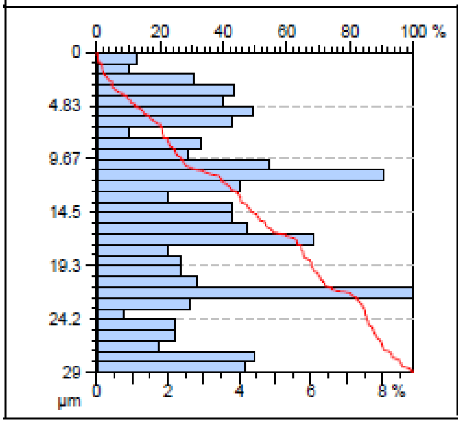

ISO 4287			
Amplitude parameters - Roughness profile			
Rp	0.937	µm	*Gaussian filter, 0.8 mm*
Rv	0.780	µm	*Gaussian filter, 0.8 mm*
Rz	1.72	µm	*Gaussian filter, 0.8 mm*
Rc	0.920	µm	*Gaussian filter, 0.8 mm*
Rt	1.72	µm	*Gaussian filter, 0.8 mm*
Ra	0.394	µm	*Gaussian filter, 0.8 mm*
Rq	0.461	µm	*Gaussian filter, 0.8 mm*
Rsk	0.242		*Gaussian filter, 0.8 mm*
Rku	2.00		*Gaussian filter, 0.8 mm*
Material Ratio parameters - Roughness profile			
Rmr	49.5	%	*c = 1 µm under the highest peak, Gaussian filter, 0.8 mm*
Rdc	0.954	µm	*p = 20%, q = 80%, Gaussian filter, 0.8 mm*